



State-of-the-Art Reactor Consequence Analyses (SOARCA) Project:

Uncertainty Analysis Plan Recommended by Sandia Technical Staff- DRAFT

Prepared by: Patrick D. Mattie*, Donald A. Kalinich, and Shawn P. Burns

Reactor Modeling & Analysis
Nuclear Energy & Global Security Technologies
Sandia National Laboratories
Albuquerque, New Mexico 87185
Operated for the U.S. Department of Energy

Contributors: Randy Guantt, Nathan Bixler, Joe Jones, F. Joe Schelling, Jon Helton and
Cedric Sallaberry, Sandia National Laboratories.
Mark T. Leonard, Dycoda, LLC.

Document Date: 10/19/2010

*Contact: Patrick D. Mattie – Org. 6762
Sandia National Laboratories
(505)284-4796 / pdmatti@sandia.gov

E/23



[THIS PAGE INTENTIONALLY LEFT BLANK]



Section 1.0 Introduction

On July 12, 2010 the Nuclear Regulatory Commission (NRC) project management for the State-of-the-Art Reactor Consequence Analyses (SOARCA) project requested that Sandia National Laboratories (SNL) technical staff prepare recommendations for an uncertainty analysis that could be executed in time to inform public meetings planned at that time for January, 2011. This report details the resulting recommendations and supporting technical basis. It should be emphasized that this is a draft plan that may be modified after further consultation with NRC technical staff and management and feedback from the SOARCA peer reviewers.

The goal of this uncertainty study is to confirm the robustness of the SOARCA predication of the most likely outcomes, and to develop insight into the overall sensitivity of the SOARCA results to uncertainty in key modeling inputs. This initial study will leverage existing models and software, along with a representative set of uncertain parameters to evaluate the method and feasibility of conducting a uncertainty analysis and will benefit a longer term study by identifying areas requiring more focused effort [1, Tasks 9, 10, 11, and 12]. The principal elements of the SNL technical staff recommendations are described briefly in the following list. A more comprehensive discussion of these recommendations and their associated technical basis is provided in the subsequent sections of this report.

Recommendation 1: The SOARCA Peach Bottom Unmitigated Long-term Station Blackout (PB LTSBO) scenario should be used to develop insight into the overall sensitivity of the SOARCA analysis to the input uncertainty.

Formally, the SOARCA proposal specifies the exploration of input uncertainty sensitivity for a single accident scenario examined as part of the SOARCA project [1] but this limitation is also consistent with the schedule constraints placed on this analysis effort. Additional support for the selection of the PB LTSBO is provided in Section 2.1.

Recommendation 2: Uncertain parameters and their associated uncertainty distributions should be identified by senior SNL and NRC technical staff based on their expert judgment and detailed knowledge of the SOARCA project.

In general a formal expert judgment elicitation process [18] involving a large number of topical area experts would provide more robust uncertainty distribution estimates. However, the resource and schedule constraints of this uncertainty analysis effort make the execution of a more formal process infeasible. Recommendation for the specific parameters to be studied and their associated distributions are provided in Section 2.2 and Section 4 respectively.



Recommendation 3: An “inner weather loop” approach which isolates the influence of weather uncertainty from other uncertainties should be employed to evaluate the overall sensitivity to input uncertainty.

Although an alternative “outer weather loop” approach has also been considered by SNL and NRC staff, it is the judgment of the SNL technical staff that the “inner weather loop” approach will promote the direct comparison to the published SOARCA best estimate results as well as allow for better resolution of the effects of input uncertainty on both the source term results and the consequence results. The peer review committee also recommended the “inner weather loop” approach (supplemented by a limited exploration of the “outer weather loop” approach, which has been completed). Detailed discussions of the treatment of uncertainty in complex systems and the SOARCA probabilistic analysis methodology are provided in Sections 2.3 and 2.4 respectively. How the treatment of uncertainty determines the overall software structure used for the analysis is discussed in Section 3.

Section 2.0 Approach

2.1 Scenario Selection

Sandia recommends the Peach Bottom Unmitigated Long Term Station Blackout (LTSBO) Scenario as the accident scenario used to develop insight into the overall sensitivity of the SOARCA analysis to uncertainty in key inputs. The justifications for this choice are both technical and programmatic:

1. The performance of the SRV as it impacts MSL failure in the LTSBO scenario was an important sensitivity study identified by the peer review committee.
2. Several implied and explicit commitments have been made by SNL and NRC staff to further explore this issue in the uncertainty analysis.
3. The LTSBO release timing and consequences are characteristic of the majority of the SOARCA scenarios, i.e., long release timing relative to evacuation time and correspondingly small off-site consequences. This makes the choice of the LTSBO consistent with the objectives of the SOARCA project to explore the center of the risk distribution as opposed to a more outlying case such as the Surry ISLOCA or SGTR.
4. The Peach Bottom LTSBO has already been the subject of an earlier uncertainty quantification pilot study. As a result a number of uncertain parameters and associated distributions have already been explored by the NRC/SNL technical team.
5. The Peach Bottom MELCOR model has proven to be robust which will lead to fewer failed MELCOR simulations and better statistics for the uncertainty study.

It should be noted that while Task Order Agreement #N6306, Rev.3 [1], only prescribes that a single scenario be investigated for the uncertainty characterization effort. Perhaps



more limiting is that the proposed time frame does not allow for a comprehensive uncertainty characterization that includes all scenarios. In this respect, the PB LTSBO scenario is sufficient in that the risk of trying to analyzing two scenarios could not be justified since two scenarios would not yield a significantly better understanding of the uncertainty. In addition, much of the off-site consequences are controlled by evacuation planning which are largely the same for all scenarios. Lastly, the selected scenario has been evaluated in great detail and was used in the preliminary scoping uncertainty analysis conducted earlier this summer, which greatly minimizes the likelihood for unknown computational issues which could put the activity at risk given the proposed schedule constraints.

2.2 Uncertain Parameters

For the uncertainty study a set of fifteen MELCOR parameters and twelve independent MACCS2 parameters have been selected. A discussion of the selected parameters is provided in Sections 4.1 and 4.2 for the MELCOR and MACCS2 parameters respectively. Table 2.2-1 lists the uncertain parameters. (Note that some of the MACCS2 parameters listed in Table 2.2-1 contain multiple sub-parameters, and thus actually denote a set of parameters.)

Table 2.2-1. SOARCA Uncertain Parameters

SOARCA Uncertain Parameters	
MELCOR	MACCS2
<i>In-Vessel Accident Progression Parameters</i>	
SRV Stochastic Failure to Reclose	Linear Coefficient in Washout Model
Battery Duration	Dry Deposition Velocities
Zr melt breakout temperature	Shielding Parameters
Molten clad drainage rate	Early Health Effects
SRV thermal seizure criterion	Dispersion Parameters
SRV open area fraction	Habitability
Steam line creep rupture	Groundshine
Fuel Failure Criterion	Hotspot relocation (dose, time)
Radial debris relocation time constants	Normal relocation (dose, time)
<i>Ex-Vessel Accident Progression Parameters</i>	
Debris lateral relocation – cavity spillover and spreading rate	Evacuation delay (chorts 1 – 5)
	Evacuation speed (chorts 1 – 5)
<i>Containment Behavior Parameters</i>	
Containment over-pressure failure	Weather Trials
DW liner failure flow area	
Hydrogen ignition criteria (where flammable)	
Railroad door open fraction (inner/outer)	
<i>Chemical Forms of Iodine and Cesium</i>	
Iodine fraction (RN04)	

2.3 Treatment of Uncertainty



In the design and implementation of analyses for complex systems, it is useful to distinguish between two types of uncertainty: aleatory uncertainty and epistemic uncertainty [2-14].

Aleatory uncertainty arises from an inherent randomness in the properties or behavior of the system under study. For example, the weather conditions at the time of a reactor accident are inherently random with respect to our ability to predict the future. Other potential examples include the variability in the properties of a population of system components and the variability in the possible future environmental conditions that a system component could possibly be exposed to. Alternative designations for aleatory uncertainty include variability, stochastic, irreducible and type A.

Epistemic uncertainty¹ derives from a lack of knowledge about the appropriate value to use for a quantity that is assumed to have a fixed value in the context of a particular analysis. For example, the pressure at which a given reactor containment would fail for a specified set of pressurization conditions is fixed but not amenable to being unambiguously defined. Other possible examples include minimum voltage required for the operation of a system and the maximum temperature that a system can withstand before failing. Alternative designations for epistemic uncertainty include state of knowledge, subjective, reducible and type B.

The analysis of a complex system typically involves answering the following three questions about the system:

- What can happen? (Q1)
- How likely is it to happen? (Q2)
- What are the consequences if it happens? (Q3)

and one additional question about the analysis itself:

- How much confidence exists in the answers to the first three questions? (Q4)

The answers to Questions (Q1) and (Q2) involve the characterization of aleatory uncertainty, and the answer to Question (Q4) involves the characterization of epistemic uncertainty. The answer to Question (Q3) typically involves numerical modeling of the system conditional on specific realizations of aleatory and epistemic uncertainty. The posing and answering of Questions (Q1)-(Q3) gives rise to what is often referred to as the Kaplan/Garrick ordered triple representation for risk [13].

¹ Strictly speaking, some parameters may have both aleatory and epistemic attributes, but be treated as epistemic for analytic convenience.

While not arbitrary, the definitions of aleatory and epistemic uncertainty do depend in a fundamental way on the system under study. This is the fundamental concept relating to the recommendation that the “inner weather loop” approach be taken to evaluating the uncertainty in the SOARCA best estimate consequence calculations (Recommendation 3). Figure 2.3.1 provides a graphical description of the difference between an “inner” and “outer” weather loop in the context of the SOARCA accident progression and off-site consequence calculations.

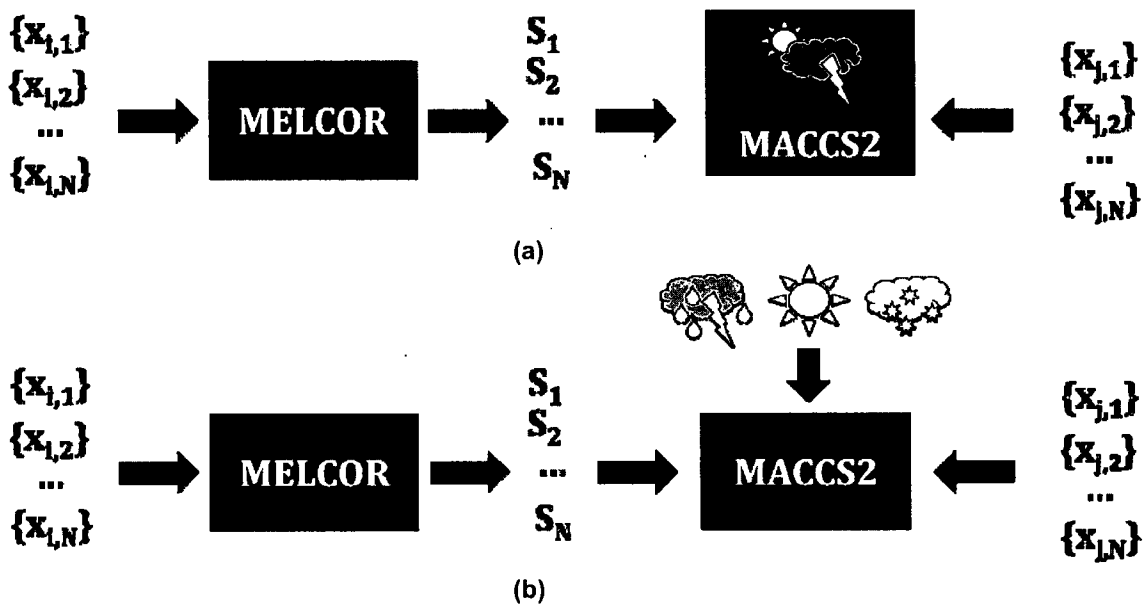


Figure 2.3.1 – Inner (a) versus outer (b) weather looping in the context of the SOARCA uncertainty quantification analysis where $x_{i,k}$ is the k^{th} instance of the MELCOR epistemic input vector x_i and $x_{j,k}$ is the k^{th} instance of the MACCS2 epistemic input vector x_j . S_k is the source term output from MELCOR which is an intermediate result.

In the modeling system used to generate the SOARCA best estimate results, weather is treated as an aleatory parameter. Each best estimate calculation represents the mean off-site consequence for a given accident sequence calculated from a large number of weather trials. In this way, the SOARCA best estimate calculation seeks an answer to the question, “What is the expected consequence of a given accident scenario, e.g., a long term station blackout, at the Peach Bottom site?” (i.e., expected outcome over all aleatory sequences) as opposed to, “What is the expected consequence of a given accident scenario during a snow storm in February at the Peach Bottom site?” (i.e., results conditional on a specific weather trail). While it is certainly feasible to obtain a reasonable estimate of the consequences of a long term station blackout at the Peach Bottom site during any given weather scenario, in the context of the SOARCA best estimate modeling system, this would not be a useful result. In the SOARCA best estimate modeling system, it is not known what the weather conditions might be during



such an event and no amount of additional information will serve to reduce that uncertainty.

Since weather represents an aleatory parameter in the SOARCA best estimate model system, it must be treated in the same way to quantify the uncertainty in that modeling system. This leads to the recommendation to use an “inner weather loop” when quantifying uncertainty in the SOARCA best estimate calculations. The “outer weather loop” would be more appropriately applied to evaluating the uncertainty in a best estimate modeling approach that did not consider weather uncertainty. In other words, the “outer weather loop” evaluates the uncertainty of a modeling system that was not used to derive the SOARCA best estimate results.

Considered in a different way, the “inner weather loop” used to obtain the SOARCA best estimate results removes weather from the epistemic parameter space all together. Since the SOARCA best estimate is not conditional on the weather trials, and the mean result represents the average over the aleatory uncertainty (weather conditions).

The SOARCA “best estimate” consequences including weather uncertainty is illustrated in Figure 2.3.2. A single source term release S_{BE} dependent upon the best estimate input, $x_{i, BE}$, was used as input to a consequence analysis dependent upon the best estimate input, $y_{i, BE}$. The result is a distribution of consequences conditional on the best estimate values (Q3), over the weather variability (Q1 and Q2). The mean value, $\|H\|$, is the mean of the CCDF and is the mean consequence over the weather variability. However, to address Q4 (How much confidence exists in the answer to the first three questions?), a series of analyses must be conducted that quantify the effects of epistemic uncertainty in the system over all possible weather conditions. These concepts are detailed in a mathematical description of the probabilistic analysis in the following section.

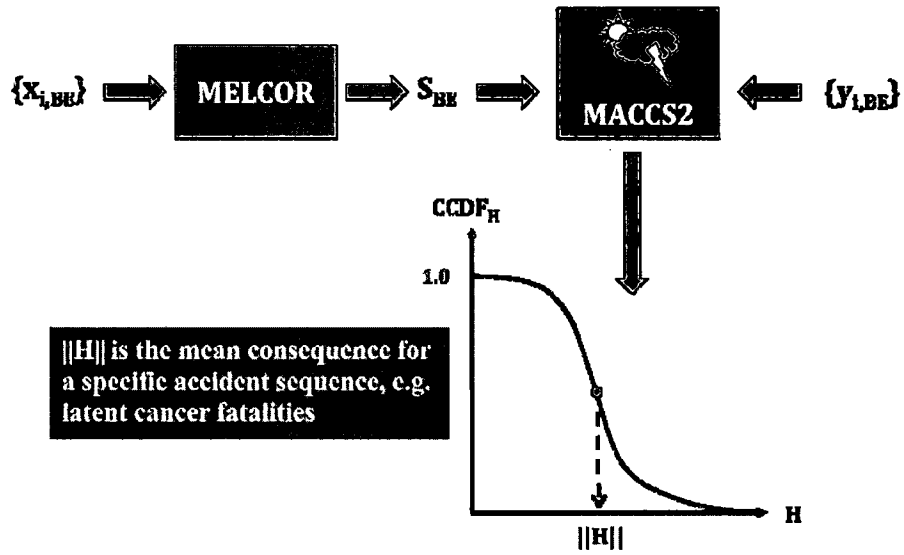


Figure 2.3.2: Typical CCDF of Consequence



2.4 Description of the Probabilistic Analysis Methodology for SOARCA

As described in Sect. 2.3, a consequence analysis for a nuclear power plant, or in general any type of engineered facility, is an analysis intended to answer three questions about the facility (i.e., Q1, Q2 and Q3) and one question about the analysis itself (i.e., Q4).

In turn, answering the four indicated questions leads to an analysis based on three basic mathematical structures or entities: EN1, a probability space characterizing aleatory uncertainty; EN2, a function that predicts the physical behavior of the facility under consideration; and EN3, a probability space characterizing epistemic uncertainty [15;16]. The probability space corresponding to EN1 characterizes aleatory uncertainty and provides the basis for answering Questions Q1 and Q2. In practice, the function corresponding to EN2 is one or more very complex numerical models and provides the basis for answering Question Q3. The probability space corresponding to EN3 characterizes epistemic uncertainty and provides the basis for answering Question Q4. The nature of the basic analysis components EN1, EN2 and EN3 in the context of the SOARCA uncertainty analysis is elaborated on in this section.

The first entity, EN1, corresponds to a probability space $(\mathcal{A}, \mathbb{A}, p_A)$, where \mathcal{A} is the set of everything that could occur in the particular universe under consideration (i.e., over some specified time period for the facility under analysis), \mathbb{A} is a suitably restricted set of subsets of \mathcal{A} for which probability is defined, and p_A is the function that defines probability for elements of \mathbb{A} (i.e., if \mathcal{S} is an element of \mathbb{A} , then $p_A(\mathcal{S})$ is the probability of \mathcal{S}) ([43], Sect. IV.3). In the usual terminology of probability theory, \mathcal{A} is called the sample space or sometimes the universal set; elements of \mathcal{A} are called elementary events; elements of \mathbb{A} are called events; p_A is called a probability measure; and $p_A(\mathcal{S})$ is the probability of the event \mathcal{S} . Elements of \mathcal{A} are often called futures; elements of \mathbb{A} are often called scenarios or scenario classes; and $p_A(\mathcal{S})$ is the probability of a scenario \mathcal{S} .

For nuclear power plants, the probability space $(\mathcal{A}, \mathbb{A}, p_A)$ for aleatory uncertainty is usually defined to characterize the occurrence of potential future events over some time period of interest (e.g., for a time period corresponding to one year plant operation or perhaps the intended operating life of the plant) that could affect the behavior/performance of the plant. Specifically, each element \mathbf{a} of the sample space \mathcal{A} is a vector of the form $\mathbf{a} = [a_1, a_2, \dots, a_n]$, where the elements of \mathbf{a} characterize the properties of one potential sequence of occurrences over the time interval under consideration. The



probability space $(\mathcal{A}, \mathbb{A}, p_A)$, for aleatory uncertainty is typically developed with extensive use of fault and event trees to define the probabilities of all possible scenarios,

For the SOARCA analysis, \mathcal{A} corresponds to the set of all possible five day sequences of weather conditions that could potentially occur at the PB site. Specifically,

$$\mathcal{A} = \{\mathbf{a} = \text{vector characterizing 5 day sequence of weather conditions at PB site}\}. \quad (2.4.1)$$

In a full consequence analysis for a nuclear power station, the indicated vector of weather conditions would be only one of many components of each element of \mathcal{A} (e.g., see summary of the NUREG-1150 reactor consequence analyses in Ref. [44]). In the SOARCA analyses, weather bins (i.e., sets of weather sequences with similar characteristics) correspond to elements of the set \mathbb{A} . Further, the probabilities that are defined by the function p_A are approximated on the basis on one year of hourly weather data collected at the PB site (i.e., if \mathcal{WB} is a weather bin, then $p_A(\mathcal{WB})$ is the probability of this weather bin, with this probability being approximated on the basis of one year of weather data).

Although the concept of a probability space is important conceptually and convenient notationally, calculations involving a probability space $(\mathcal{A}, \mathbb{A}, p_A)$ are often described with a density function $d_A(\mathbf{a})$, where

$$p_A(\mathcal{S}) = \int_{\mathcal{S}} d_A(\mathbf{a}) d\mathcal{S} \quad (2.4.2)$$

for $\mathcal{S} \in \mathbb{A}$, $\mathbf{a} \in \mathcal{S}$, and $d\mathcal{S}$ corresponding to an increment of volume from \mathcal{S} . Then, the expected value, variance, cumulative distribution function (CDF), and complementary cumulative distribution function (CCDF) at time τ (yr) associated with a real-valued function $y = f(\tau|\mathbf{a})$ defined on \mathcal{A} are defined by

$$E_A[f(\tau|\mathbf{a})] = \int_{\mathcal{A}} f(\tau|\mathbf{a}) d_A(\mathbf{a}) d\mathcal{A}, \quad (2.4.3)$$

$$V_A[f(\tau|\mathbf{a})] = \int_{\mathcal{A}} \{f(\tau|\mathbf{a}) - E_A[f(\tau|\mathbf{a})]\}^2 d_A(\mathbf{a}) d\mathcal{A}, \quad (2.4.4)$$

$$p_A[f(\tau|\mathbf{a}) \leq y] = \int_{\mathcal{A}} \delta_y[f(\tau|\mathbf{a})] d_A(\mathbf{a}) d\mathcal{A}, \quad (2.4.5)$$

and

$$p_A[y \leq f(\tau|\mathbf{a})] = \int_{\mathcal{A}} \bar{\delta}_y[f(\tau|\mathbf{a})] d_A(\mathbf{a}) d\mathcal{A}, \quad (2.4.6)$$



respectively, where

$$\underline{\delta}_y[f(\tau|\mathbf{a})] = \begin{cases} 1 & \text{if } f(\tau|\mathbf{a}) \leq y \\ 0 & \text{otherwise,} \end{cases} \quad \bar{\delta}_y[f(\tau|\mathbf{a})] = \begin{cases} 1 & \text{if } f(\tau|\mathbf{a}) > y \\ 0 & \text{otherwise,} \end{cases}$$

and dA represents an increment of volume from A .

The equalities in Eqs. (2.4.5) and (2.4.6) in effect define a cumulative distribution function (CDF) and a complementary cumulative distribution function (CCDF), respectively. Specifically, if $[y_{mn}, y_{mx}]$ includes the range of possible values for y , then the plots defined by the points

$$\{y, p_A[f(\tau|\mathbf{a}) \leq y]\} \text{ and } \{y, p_A[y < f(\tau|\mathbf{a})]\} \quad (2.4.7)$$

for $y_{mn} \leq y \leq y_{mx}$ correspond to the CDF and CCDF, respectively, for y . A CCDF is defined in Eq. (2.4.6) because of the typical usage of CCDFs to represent uncertainty in risk assessments. In particular, a CCDF answers the question “How likely is it to be this bad or worse?”, which is usually the question asked with respect to individual consequences in a risk assessment. In particular, CCDFs constitute the standard uncertainty structure used in the presentation of off-site consequence results calculated with MACCS.

The second entity, EN2, corresponds to a model, or more realistically a large system of interacting models, that predict the behavior of a nuclear power plant under accident conditions and various summary measures of this behavior (e.g., radionuclide release rates). Notationally, this model can be represented by a function of the form

$$\mathbf{f}(\tau|\mathbf{a}) = [f_1(\tau|\mathbf{a}), f_2(\tau|\mathbf{a}), \dots, f_m(\tau|\mathbf{a})], \quad (2.4.8)$$

where τ corresponds to time (yr), each element $f_j(\tau|\mathbf{a})$ of $\mathbf{f}(\tau|\mathbf{a})$ is a specific calculated result, and \mathbf{a} is an element of the sample space A for aleatory uncertainty. In general, the value of $\mathbf{f}(\tau|\mathbf{a})$, and indeed the actual structure of the individual models that are combined to produce $\mathbf{f}(\tau|\mathbf{a})$, will change with changing values for \mathbf{a} . In the SOARCA uncertainty analysis, the function $\mathbf{f}(\tau|\mathbf{a})$ corresponds to combined calculations performed with models implemented within the MELCOR and MACCS2 programs. Consistent with the notation used in Eq. (2.4.8), the indicated models produce a large number of time dependent results.

In practice, functions of the form indicated in Eq. (2.4.8) are usually too complex for quadrature-based evaluations. This is certainly the case for results obtained with



MACCS2 due to the complexity of the conditions associated with weather sequences and the extensive calculations that underlie the estimation of off-site consequences. As a consequence, results of the form indicted in Eqs. (2.4.3)-(2.4.6) are usually estimated with some form of sampling procedure. One possibility is to use simple random sampling from the sample space \mathcal{A} for aleatory uncertainty. With this approach, a random sample

$$\mathbf{a}_j = [a_{1j}, a_{2j}, \dots, a_{nj}], j = 1, 2, \dots, nSA, \quad (2.4.9)$$

is generated from \mathcal{A} consistent with the defining probabilities for the probability space $(\mathcal{A}, \mathbb{A}, p_A)$. Then, the results in Eqs. (2.4.3)-(2.4.6) are approximated on the basis of this sample. For example, the approximations to the expected value in Eq. (2.4.3) and the exceedance probability in Eq. (2.4.6) for an element $f(\tau|\mathbf{a})$ of the function $\mathbf{f}(\tau|\mathbf{a})$ in Eq. (2.4.8) are

$$E_A [f(\tau|\mathbf{a})] \cong \sum_{j=1}^{nSA} f(\tau|\mathbf{a}_j) / nSA \quad (2.4.10)$$

and

$$p_A [y \leq f(\tau|\mathbf{a})] \cong \sum_{j=1}^{nSA} \delta_y [f(\tau|\mathbf{a}_j)] / nSA, \quad (2.4.11)$$

respectively.

An alternate procedure is to subdivide \mathcal{A} into a sequence of disjoint subsets $\mathcal{A}_j, j = 1, 2, \dots, nSA$, and randomly sample a single element \mathbf{a}_j from each set \mathcal{A}_j . Then, the results in Eqs. (2.4.3)-(2.4.6) are approximated on the basis of the sets \mathcal{A}_j and the sampled elements \mathbf{a}_j . For example, the resultant approximations to the expected value in Eq. (2.4.3) and the exceedance probability in Eq. (2.4.6) for an element $f(\tau|\mathbf{a})$ of the function $\mathbf{f}(\tau|\mathbf{a})$ in Eq. (2.4.8) are:

$$E_A [f(\tau|\mathbf{a})] \cong \sum_{j=1}^{nSA} f(\tau|\mathbf{a}_j) p_A(\mathcal{A}_j) \quad (2.4.12)$$

and

$$p_A [y \leq f(\tau|\mathbf{a})] \cong \sum_{j=1}^{nSA} \delta_y [f(\tau|\mathbf{a}_j)] p_A(\mathcal{A}_j), \quad (2.4.13)$$

respectively. This approach corresponds to use of the Kaplan-Garrick ordered triple representation for risk.



A variant of the approach indicated in the preceding paragraph is used with MACCS2 in the SOARCA analyses in the estimation of expected values and exceedance probabilities. In this variant, the sets $\mathcal{A}_j, j = 1, 2, \dots, nSA$, correspond to $\mathcal{WB}_j, j = 1, 2, \dots, 36 = nWB$, weather bins (i.e., subsets of the set \mathcal{A} in Eq.(2.4.1)), and $\mathbf{a}_{jk}, k = 1, 2, \dots, nWB_j$, elements are sampled from each weather bin \mathcal{WB}_j . In the SOARCA uncertainty analyses, nWB_j is defined by

$$nWB_j = \begin{cases} [0.05 nWB_j] & \text{if } 12 < 0.05 nWB_j \\ 12 & \text{if } 0.05 nWB_j < 12 < nWB_j \\ nWB_j & \text{if } nWB_j \leq 12, \end{cases} \quad (2.4.14)$$

where nWB_j is the number of elements in \mathcal{WB}_j estimated on the basis of one year of weather data and $[~]$ corresponds to the greatest integer function. Then, the results in Eqs. (2.4.3)-(2.4.6) are approximated on the basis of the sets \mathcal{WB}_j and the sampled elements \mathbf{a}_{jk} . For example, the resultant approximations to the expected value in Eq. (2.4.3) and the exceedance probability in Eq. (2.4.6) for an element $f(\tau|\mathbf{a})$ of the function $\mathbf{f}(\tau|\mathbf{a})$ in Eq. (2.4.8) are

$$E_A [f(\tau|\mathbf{a})] \cong \sum_{j=1}^{nWB} \left[\sum_{k=1}^{nWB_j} f(\tau|\mathbf{a}_{jk}) / nWB_j \right] p_A(\mathcal{WB}_j) \quad (2.4.15)$$

and

$$p_A [y \leq f(\tau|\mathbf{a})] \cong \sum_{j=1}^{nWB} \left\{ \sum_{k=1}^{nWB_j} \delta_y [f(\tau|\mathbf{a}_{jk})] / nWB_j \right\} p_A(\mathcal{WB}_j), \quad (2.4.16)$$

respectively.

The third entity, EN3, corresponds to a probability space $(\mathcal{E}, \mathbb{E}, p_E)$ for epistemic uncertainty. The conceptual properties associated with probability space $(\mathcal{E}, \mathbb{E}, p_E)$ are the same as indicated in Eqs. (2.4.2)-(2.4.6) for the probability space $(\mathcal{A}, \mathbb{A}, p_A)$ for aleatory uncertainty. In general, the elements of the sample space \mathcal{E} are vectors of the form:



$$\begin{aligned}\mathbf{e} &= [\mathbf{e}_A, \mathbf{e}_M] \\ &= [e_{A1}, e_{A2}, \dots, e_{A,nEA}, e_{M1}, e_{M2}, \dots, e_{M,nEM}] \\ &= [e_1, e_2, \dots, e_{nE}], nE = nEA + nEM,\end{aligned}\tag{2.4.17}$$

where $\mathbf{e}_A = [e_{A1}, e_{A2}, \dots, e_{A,nEA}]$ is a vector of epistemically uncertain quantities used in the characterization of aleatory uncertainty (not considered in this analysis as no aspect of the weather trials are treated as being epistemically uncertain) and $\mathbf{e}_M = [e_{M1}, e_{M2}, \dots, e_{M,nEM}]$ is a vector of epistemically uncertain quantities used in the evaluation of $\mathbf{f}(\tau|\mathbf{a})$.

In the SOARCA uncertainty analysis, the vector \mathbf{e}_M of epistemically uncertain model parameters has two components: a vector \mathbf{e}_{ME} of epistemically uncertain parameters used in MELCOR calculations and a vector \mathbf{e}_{MA} of epistemically uncertain parameters used in MACCS2 calculations (Table 2.2-1). Specifically, the form of \mathbf{e}_M in the SOARCA uncertainty analysis is

$$\begin{aligned}\mathbf{e}_M &= [\mathbf{e}_{ME}, \mathbf{e}_{MA}] \\ &= [e_{ME,1}, e_{ME,2}, \dots, e_{ME,nME}, e_{MA1}, e_{MA2}, \dots, e_{MA,nMA}] \\ &= [e_1, e_2, \dots, e_{nE}], nE = nME + nMA\end{aligned}\tag{2.4.18}$$

with $nME = 12$ and $nMA = 9$.

In practice, the probability space $(\mathcal{E}, \mathbb{E}, p_E)$ is defined by assigning probability distributions to the individual elements of \mathbf{e} . In addition, correlations and other restrictions involving the elements of \mathbf{e} may also be specified. The specified distributions serve as mathematical summaries of all available information with respect to where the appropriate values for the elements of \mathbf{e} are located and are often developed through expert review processes [18-27]. The development of the distributions characterizing epistemic uncertainty in the SOARCA uncertainty analysis are discussed in Sect. 4.1.

With the introduction of the probability space $(\mathcal{E}, \mathbb{E}, p_E)$ for epistemic uncertainty, the representation for the system model in Eq. (2.4.8) becomes

$$\mathbf{f}(\tau|\mathbf{a}, \mathbf{e}_M) = [f_1(\tau|\mathbf{a}, \mathbf{e}_M), f_2(\tau|\mathbf{a}, \mathbf{e}_M), \dots, f_m(\tau|\mathbf{a}, \mathbf{e}_M)].\tag{2.4.19}$$

Further, given that there is no uncertainty in the characterization of aleatory uncertainty as is the case in the SOARCA analysis, results of the form in Eqs.(2.4.3), (2.4.5) and (2.4.6) become:



$$E_A[f(\tau|\mathbf{a}, \mathbf{e}_M)] = \int_{\mathcal{A}} f(\tau|\mathbf{a}, \mathbf{e}_M) d_A(\mathbf{a}) dA, \quad (2.4.20)$$

$$p_A[f(\tau|\mathbf{a}, \mathbf{e}_M) \leq y] = \int_{\mathcal{A}} \delta_y[f(\tau|\mathbf{a}, \mathbf{e}_M)] d_A(\mathbf{a}) dA, \quad (2.4.21)$$

and

$$p_A[y < f(\tau|\mathbf{a}, \mathbf{e}_M)] = \int_{\mathcal{A}} \bar{\delta}_y[f(\tau|\mathbf{a}, \mathbf{e}_M)] d_A(\mathbf{a}) dA, \quad (2.4.22)$$

where $f(\tau|\mathbf{a}, \mathbf{e}_M)$ corresponds to one of the functions $f_j(\tau|\mathbf{a}, \mathbf{e}_M)$ contained in $\mathbf{f}(\tau|\mathbf{a}, \mathbf{e}_M)$. As \mathbf{e}_M changes, each of the preceding quantities also changes and has a probability distribution that derives from the probability space $(\mathcal{E}, \mathbb{E}, p_E)$ for epistemic uncertainty.

In concept, probability distributions over epistemic uncertainty for quantities of the form defined in Eqs. (2.4.20)-(2.4.22) are defined by integrals over the sample space \mathcal{E} for epistemic uncertainty. In practice, such integrals are too complex for quadrature approximations and, as a consequence, must be approximated with sampling-based procedures. Specifically, a random or Latin hypercube sample [28;29]

$$\mathbf{e}_{Mi} = [e_{i1}, e_{i2}, \dots, e_{i,nE}], i = 1, 2, \dots, nSE, \quad (2.4.23)$$

is generated from \mathcal{E} in a manner consistent with the probability distributions that characterize epistemic uncertainty. Then, analysis results of interest (e.g., results of the form in Eqs. (2.4.20-2.4.22)) are determined for each element \mathbf{e}_{Mi} of the indicated sample. For example, if random sampling is used to approximate integrals over aleatory uncertainty as in Eqs. (2.4.10) and (2.4.11), the approximations to the results in Eqs. (2.4.20) and (2.4.22) become:

$$\begin{aligned} E_A[f(\tau|\mathbf{a}, \mathbf{e}_{Mi})] &= \int_{\mathcal{A}} f(\tau|\mathbf{a}, \mathbf{e}_{Mi}) d_A(\mathbf{a}) dA \\ &\cong \sum_{j=1}^{nSA} f(\tau|\mathbf{a}_j, \mathbf{e}_{Mi}) / nSA \\ &= \tilde{E}_A[f(\tau|\mathbf{a}, \mathbf{e}_{Mi})] \end{aligned} \quad (2.4.24)$$

and



$$\begin{aligned}
p_A [y < f(\tau | \mathbf{a}, \mathbf{e}_{Mi})] &= \int_{\mathcal{A}} \bar{\delta}_y [f(\tau | \mathbf{a}, \mathbf{e}_{Mi})] d_A(\mathbf{a}) d\mathbf{A} \\
&\cong \sum_{j=1}^{nSA} \bar{\delta}_y [f(\tau | \mathbf{a}_j, \mathbf{e}_{Mi})] / nSA \\
&= \tilde{p}_A [y < f(\tau | \mathbf{a}, \mathbf{e}_{Mi})]
\end{aligned} \tag{2.4.25}$$

for each element \mathbf{e}_{Mi} of the indicated sample. Approximations to distributions summarizing epistemic uncertainty can now be obtained from results of the form in Eqs. (2.4.24) and (2.4.25) with an equal weight of $1/nSE$ assigned to the results obtained with each sample element. Further, mappings of the form

$$[\mathbf{e}_{Mi}, \tilde{E}_A [f(\tau | \mathbf{a}, \mathbf{e}_{Mi})]], i = 1, 2, \dots, nSE, \tag{2.4.26}$$

and

$$[\mathbf{e}_{Mi}, \tilde{p}_A [y < f(\tau | \mathbf{a}, \mathbf{e}_{Mi})]], i = 1, 2, \dots, nSE, \tag{2.4.27}$$

form the basis for the application of a variety of sensitivity analysis procedures as discussed in Sect. 3.2.

In the SOARCA uncertainty analysis, a sample of size $nSE = 100$ is used to generate the sample indicated in Eq.(2.4.23). Specifically, the component \mathbf{e}_{ME} of \mathbf{e}_M will be sampled with random sampling and the component \mathbf{e}_{MA} of \mathbf{e}_M will be sampled with Latin hypercube sampling. In turn, SOARCA results of the form indicated in Eqs. (2.4.15) and (2.4.16) will be approximated by

$$\begin{aligned}
E_A [f(\tau | \mathbf{a}, \mathbf{e}_{Mi})] &\cong \sum_{j=1}^{nWB} \left[\sum_{k=1}^{nWB_j} f(\tau | \mathbf{a}_{jk}, \mathbf{e}_{Mi}) / nWB_j \right] p_A(\mathcal{WB}_j) \\
&= \tilde{E}_A [f(\tau | \mathbf{a}, \mathbf{e}_{Mi})]
\end{aligned} \tag{2.4.28}$$

and

$$\begin{aligned}
p_A [y \leq f(\tau | \mathbf{a}, \mathbf{e}_{Mi})] &\cong \sum_{j=1}^{nWB} \left\{ \sum_{k=1}^{nWB_j} \bar{\delta}_y [f(\tau | \mathbf{a}_{jk}, \mathbf{e}_{Mi})] / nWB_j \right\} p_A(\mathcal{WB}_j) \\
&= \tilde{p}_A [y \leq f(\tau | \mathbf{a}, \mathbf{e}_{Mi})]
\end{aligned} \tag{2.4.29}$$

for each sample element \mathbf{e}_{Mi} . As discussed in the preceding paragraph, results of the form in Eqs. (2.4.28) and (2.4.29) provided the basis in SOARCA for assessing the effects and implications of epistemic uncertainty.



Section 3.0 Code Integration and Analyses

3.1 Description of Code Integration [Wiring Diagram]

Figure 3.1.1 provides a conceptual representation of the uncertainty analysis:

- Uncertain MELCOR and MACCS2 parameters are sampled
- MELCOR is run for each set of its sampled values
- MACCS2 is run for each set of its sampled values in conjunction with the associated MELCOR source term outputs

In this section a description of the elements and processes (e.g., codes, files) used to implement the conceptual representation is provided. Figure 3.1.1 shows the information flow of the SOARCA uncertainty analysis. A description of each item in Figure 3.1.1 is described in this section.

MELCOR Uncertain Parameters: The chosen uncertain parameters in the MELCOR model for the Peach Bottom LTSBO scenario are defined by their distribution types and associated parameters (e.g., uniform distribution with a lower and upper bound) (see Section 4.1). These distributions are incorporated into the MELCOR Uncertainty Engine input template file.

MELCOR Input Deck: The input for the MELCOR model of the Peach Bottom LTSBO scenario is divided into a set of input files. The files listed in Table 3.1-1 contain the majority of the information that describe the model. The file jelly_DAK.gen uses the MELCOR R*I*F feature to incorporate the individual input files in Table 3.1-1 into one a single MELGEN² file. The file jelly_DAK.cor contains the MELCOR input information.

MELCOR Uncertainty Engine Input Template: The MELGEN/MELCOR uncertainty engine template file consists of three sections. The first section contains the uncertain parameter definitions. Also, variables are defined for each uncertain parameter. The second section contains the model's MELGEN input records. These are incorporated by using the R*I*F feature to read in the jelly_DAK.gen file. The MELGEN records which contain uncertain parameters are also located in this section of the template file. The uncertain parameters in each record are replaced by their respective variables (defined in the first section of the template file). The third section contains the model's MELCOR input

² MELCOR executes in two parts. The first is a program called MELGEN, in which most of the input is specified, processed, and checked. When the input checks are satisfied, a restart file of all the information in the MELCOR database is written for the initial conditions of the calculation. The second part of MELCOR is the MELCOR program itself, which advances the problem through time based on the database generated by MELGEN and any additional MELCOR input. See the MELCOR Users' Guide for more details.



records. These are incorporated by using the R*I*F feature to read in the jelly_DAK.cor file.

MELCOR Uncertainty Engine: Based in the input template, the MELCOR Uncertainty Engine creates N MELCOR input files. Monte Carlo sampling is used to generate N samples of the uncertain parameters. In each input file the uncertain parameter variables are replaced with their corresponding sampled value. In addition, an output file is created which contains the sampled values.

Sampled MELCOR Uncertain Parameters: The MELCOR Uncertainty Engine generates an Excel .csv file which contains the sampled uncertain parameter values.

RN Parsing Uncertainty Deck Generator: The uncertainty in the partitioning of the initial iodine core inventory between RN class 4 and RN class 16 cannot be directly implemented as a single sampled parameter value. Rather, that sampled value is an input into the core inventory calculation where it influences the masses RN classes 2, 4, 7, 16, and 17. The RN Parsing Uncertainty Deck Generator implements the inventory partitioning calculation as an Excel VBA macro in an Excel workbook. The sampled value of the fraction of the initial iodine core inventory in RN class 4 is manually copied and pasted into the Excel workbook. The macro performs the partitioning calculation for each sampled value. The results of the calculation are incorporated into the appropriate records of the dch-mdcy_mod.gen and rn_mass_midcy_mod.gen files. A separate dch-mdcy_mod.gen and rn_mass_midcy_mod.gen is created for each sampled value.

Containment Failure Uncertainty Deck Generator: The uncertainty in the mode of containment failure cannot be directly implemented as a single sampled parameter value. Rather, each containment failure mode is characterized in a separate MELGEN input file. The sampled value for the containment failure mode is used to determine which file to use in a given realization. The Containment Failure Uncertainty Deck Generator implements the containment failure mode as an Excel VBA macro in an Excel workbook. The sampled value for the containment failure mode is manually copied and pasted into the Excel workbook. The macro selects the containment failure MELGEN input file based on the containment failure mode sampled value and creates a properly named version of that for the given realization.

N MELCOR Input File Sets: A MELCOR input file is created for each set of sampled values (i.e., realization). That file incorporates the original input deck with its uncertain parameters set equal to their sampled values. For uncertainties that cannot be directly implemented as a single parameter value (e.g., fraction of initial iodine core inventory partitioned into RN class 4) additional input files are generated, which are incorporated via the R*I*F feature (see Figure 3.1.2)



MELGEN/MELCOR: The MELGEN and MELCOR executables are used to run the N MELCOR input files. Each run creates its own set of output files.

N MELCOR Output File Sets: Each MELCOR run has its own set of output files (see Figure 3.1.2).

MELMACCS Template File: The MELMACCS template file contains input needed by MELMACCS to extract the source term information from the MELCOR .ptf output files and generate the source term input files used by WinMACCS.

MELMACCS: The .ptf file from each MELCOR run is processed by MELMACCS to extract the information on the source term released to the environment and put it into a MACCS2-compatible format.

N MELMACCS Output Files: A MELMACCS output file is created from each MELCOR .ptf output file.

WinMACCS³ Uncertain Parameters: The uncertain parameters in the WinMACCS model for the Peach Bottom LTSBO scenario are defined by their distribution types and associated parameters (e.g., uniform distribution with a lower and upper bound) (see Section 4.2). These distributions are incorporated into the WinMACCS input file using the WinMACCS GUI. The distributions are sampled (using LHS) when WinMACCS is run.

WinMACCS Input File: The WinMACCS input file contains input used by WinMACCS (e.g., weather, evacuation parameters, etc.) to perform consequence calculations.

WinMACCS: WinMACCS is used to calculate consequences for the N source term inputs (from the N MELMACCS output files) in conjunction with the uncertainty in the WinMACCS parameters. Weather uncertainty (using weather bin sampling⁴) is evaluated for each source term input and associated WinMACCS uncertain parameter sample.

N WinMACCS Output Files: A WinMACCS output file is generated for each source term input.

³ WinMACCS is the GUI shell that executes MACCS2

⁴ see the MACCS2 Users Guide, Section 5.1

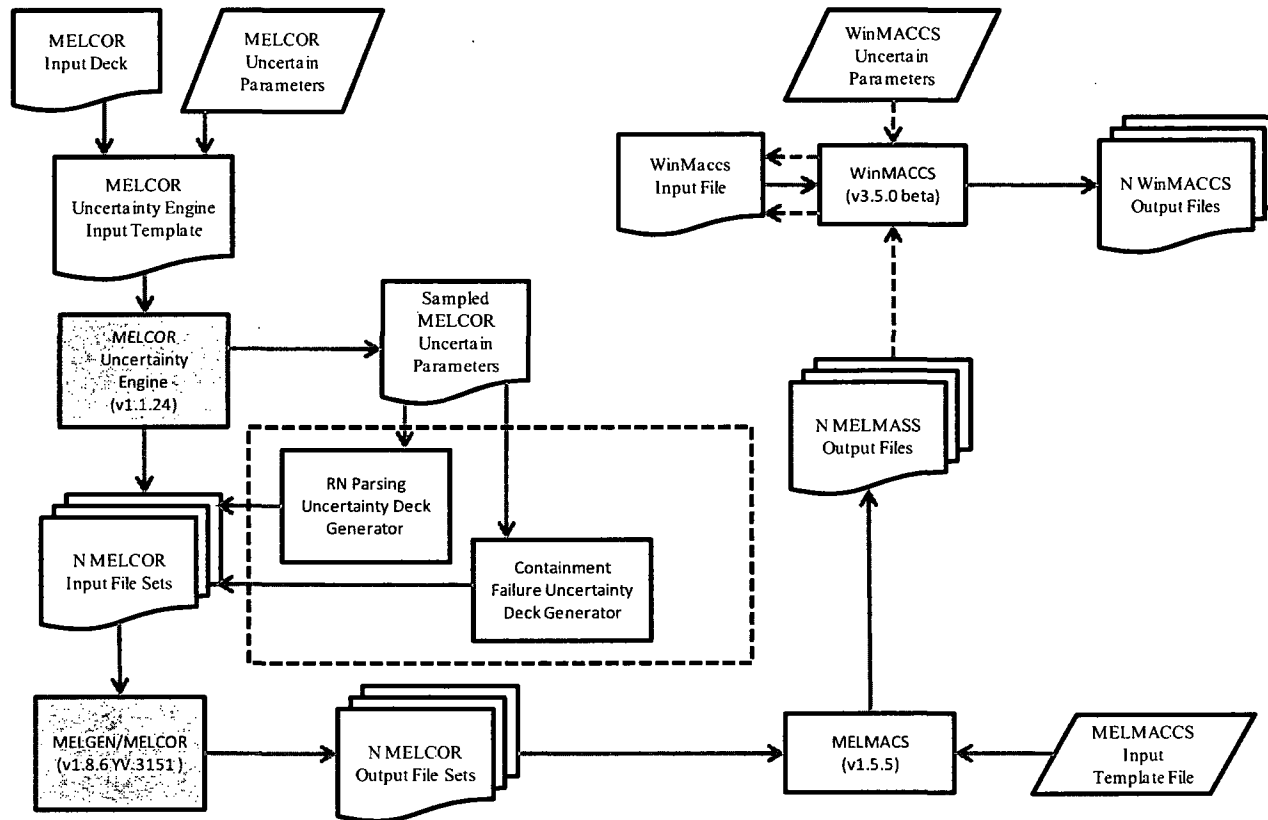


Figure 3.1.1: SOARCA Uncertainty Analysis Wiring Diagram

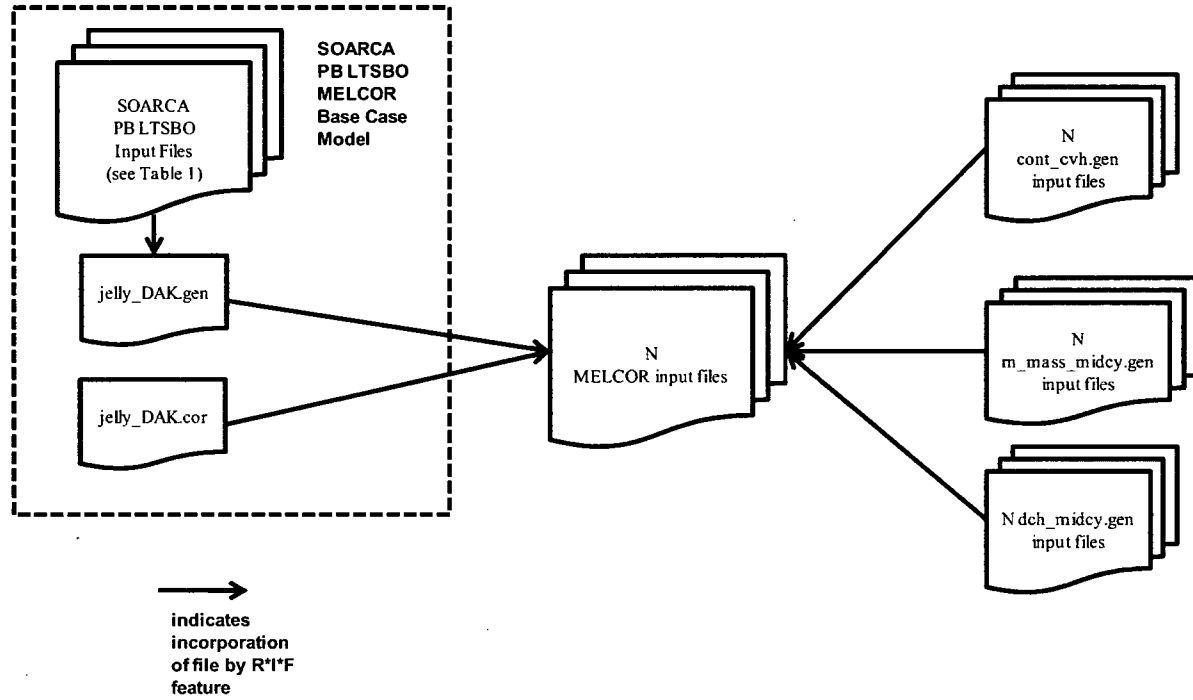


Figure 3.1.2: MELCOR Input Files



Table 3.1-1. SOARCA Peach Bottom Long-Term Station Blackout MELCOR Model Input Files

10x10-rn-set.gen	mp.gen
10x10-rpv-cvh.gen	rb-cvh.gen
10x10-rpv-fl.gen	rb-fl.gen
10x10core.gen	rb-hs-depos.gen
burn.gen	rb-hs.gen
cav.gen	rcic2.gen
cf-midcy.gen	rsc-sys.gen
cf2.gen	recirc.gen
chex-layman-midcy.gen	rhr2.gen
cont-cvh.gen	rn-cor-struc.gen
cont-cvh_mod.gen	rn-mass-midcy.gen
cont-hs.gen	rn.gen
core-sc.gen	rpv-hs.gen
cvtype.gen	seq-trip.gen
dch-midcy.gen	sloca-rcic.gen
dir.txt	sp-heatcap.gen
dw-liner-melt.gen	srv-fl2.gen
hpci.gen	srv-tailpipe.gen
hpci2.gen	Write_Output.gen
lpcs.gen	

3.2 Parameter Sensitivity and Uncertainty Analysis Methodology

Closely associated with the characterization of epistemic uncertainty provided by the probability space corresponding to EN3 and the answering of Question Q4 are the concepts of uncertainty analysis and sensitivity analysis, where uncertainty analysis designates the determination of the epistemic uncertainty in analysis results that derives from epistemic uncertainty in analysis inputs and sensitivity analysis designates the determination of the contribution of the epistemic uncertainty in individual analysis inputs to the epistemic uncertainty in analysis results. Basically, uncertainty and sensitivity analysis are the means by which EN3 gives rise to the answer to Question Q4. A number of approaches to uncertainty and sensitivity analysis exist, including differential analysis, response surface methods, variance decomposition methods, and sampling-based (i.e., Monte Carlo) methods [25-32]. A parameter uncertainty analysis will be conducted using the methods described below for both source term and radiological

consequences to evaluate the effects of the uncertainty in key inputs on the selected accent scenario [1].

Several of the approaches to sensitivity analysis that can be used in conjunction with a sampling-based uncertainty analysis are listed and briefly summarized below. In this summary, (i) x_j is an element of a vector $\mathbf{x} = [x_1, x_2, \dots, x_{nX}]$ of epistemically uncertain analysis inputs, (ii) y_k is an element of $\mathbf{y}(\mathbf{x}) = [y_1(\mathbf{x}), y_2(\mathbf{x}), \dots, y_{nY}(\mathbf{x})]$, (iii) $\mathbf{x}_i = [x_{i1}, x_{i2}, \dots, x_{i,nX}]$, $i = 1, 2, \dots, nS$, is a random or Latin hypercube sample from the possible values for \mathbf{x} generated in consistency with the joint distribution assigned to the x_j , (iv) $\mathbf{y}_i = \mathbf{y}(\mathbf{x}_i)$ for $i = 1, 2, \dots, nS$, and (v) x_{ij} and y_{ik} are elements of \mathbf{x}_i and \mathbf{y}_i , respectively.

Scatterplots. Scatterplots are plots of the points $[x_{ij}, y_{ik}]$ for $i = 1, 2, \dots, nS$ and can reveal nonlinear or other unexpected relationships (Fig. 3.2.1). In many analyses, scatterplots provide all the information that is needed to understand the sensitivity of analysis results to the uncertainty in analysis inputs. Further, scatterplots constitute a natural starting point in a complex analysis that can help in the development of a sensitivity analysis strategy using one or more additional techniques. Additional information: Sect. 6.6.1, Ref. [33]; Sect. 6.1, Ref. [32].

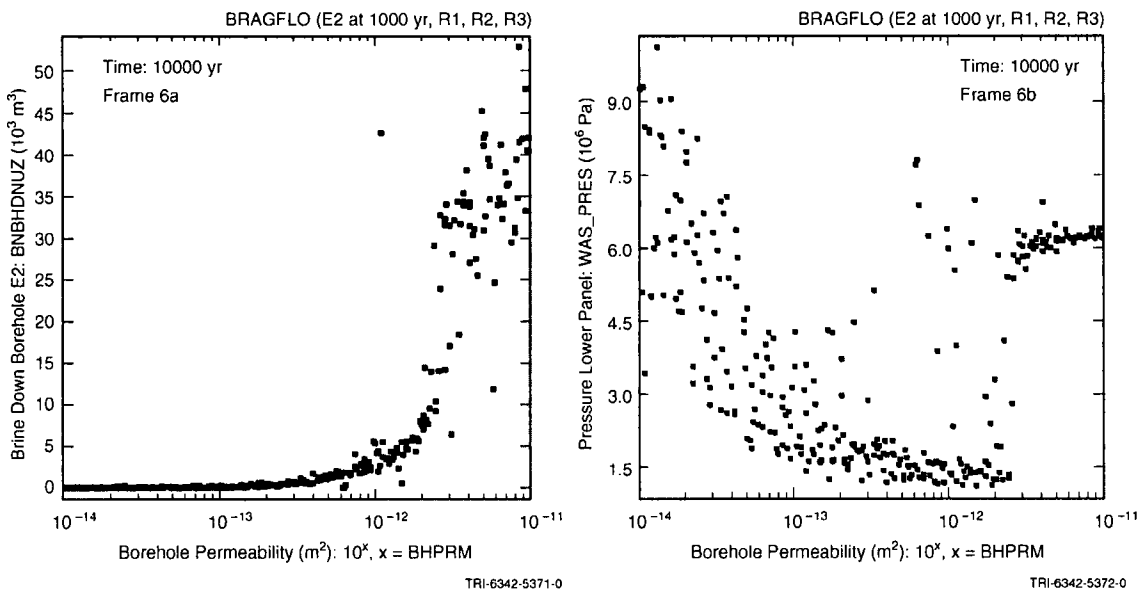


Fig.3.2.1. Examples of scatterplots obtained in a sampling-based uncertainty/sensitivity analysis (Figs. 8.1, 8.2, Ref. [34]).

Correlation. A correlation coefficient (CC) provides a measure of the strength of the linear relationship between x_j and y_k . The CC between x_j and y_k is equal to the standardized regression coefficient (SRC) in a linear regression relating y_k to x_j and is also equal in absolute value to the square root of the R^2 value associated with the indicated regression. When calculated with raw (i.e., untransformed) data, the CC is often referred to as the Pearson CC. Additional information: Sect. 6.6.4, Ref. [33]; Sect. 6.2, Ref. [32].

Regression Analysis. Regression analysis provides an algebraic representation of the relationships between y_k and one or more x_j 's. Regression analysis is usually performed in a stepwise fashion, with initial inclusion of most important x_j , then two most important x_j 's, and so on until no more x_j 's that significantly affect y_k can be identified. Variable importance is indicated by order of selection in the stepwise process, changes in R^2 values as additional variables are added to the regression model, and SRCs for the x_j 's in the final regression model (Table 3.2-1). A display of regression results in the form shown in Table 3.2-1 is very unwieldy when results at a sequence of times are under consideration. In this situation, a more compact display of regression results is provided by plotting time-dependent SRCs (Fig. 3.2.2a). Additional information: Sects. 6.6.2, 6.6.3, 6.6.5, Ref. [33]; Sect. 6.3, Ref. [32].

Table 3.2-1. Example of Stepwise Regression Analysis to Identify Uncertain Variables Affecting the Uncertainty in Pressure at 10,000 yr in Fig. 5a (Table 8.6, Ref. [34])

Step ^a	Variable ^b	SRC ^c	R^2 ^d
1	<i>WMICDFLG</i>	0.718	0.508
2	<i>HALPOR</i>	0.466	0.732
3	<i>WGRCOR</i>	0.246	0.792
4	<i>ANHPRM</i>	0.129	0.809
5	<i>SHRGSSAT</i>	0.070	0.814
6	<i>SALPRES</i>	0.063	0.818

^a Steps in stepwise regression analysis.
^b Variables listed in the order of selection in regression analysis.
^c SRCs for variables in final regression model.
^d Cumulative R^2 value with entry of each variable into regression model.

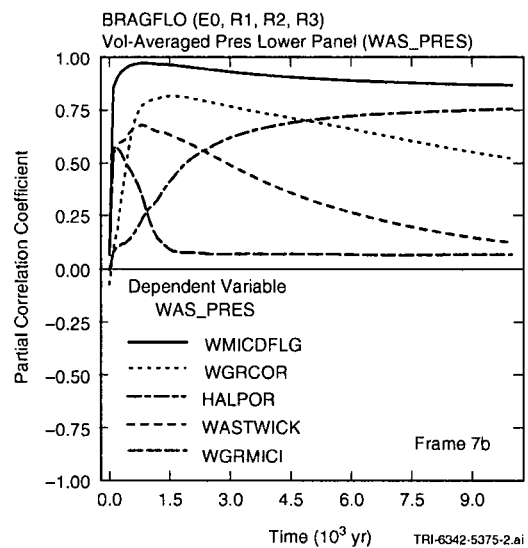
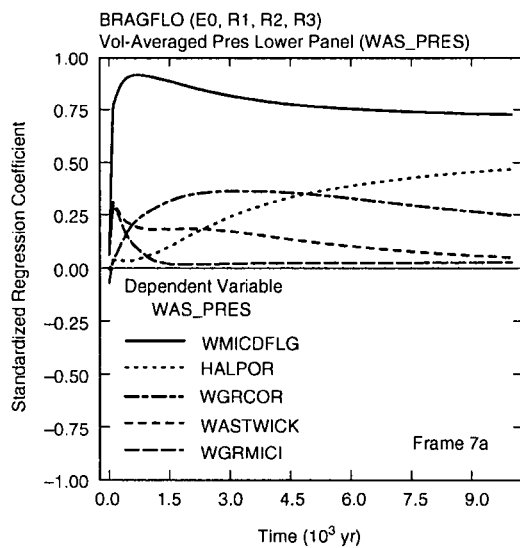




Fig. 3.2.2. Time-dependent sensitivity analysis results for uncertain pressure curves in Fig. 5a: (a) SRCs as a function of time, and (b) PCCs as a function of time (Fig. 8.3, Ref. [34]).

Partial Correlation. A partial correlation coefficient (PCC) provides a measure of the strength of the linear relationship between y_k and x_j after the linear effects of all other elements of \mathbf{x} have been removed. Similarly to SRCs, PCCs can be determined as a function of time for time-dependent analysis results (Fig. 3.2.2b). Additional information: Sect. 6.6.4, Ref. [33]; Sect. 6.4, Ref. [32].

Rank Transformations. A rank transformation replaces values for y_k and x_j with their corresponding ranks. Specifically, the smallest value for a variable is assigned a rank of 1; next largest value is assigned a rank of 2; tied values are assigned their average rank; and so on up to the largest value, which is assigned a rank of nS . Use of the rank transformation converts a nonlinear but monotonic relationship between y_k and x_j to a linear relationship and produces rank (i.e., Spearman) correlations, rank regressions, standardized rank regression coefficients (SRRCs) and partial rank correlation coefficients (PRCCs). In the presence of nonlinear but monotonic relationships between the x_j and y_k , the use of the rank transform can substantially improve the resolution of sensitivity analysis results (Table 3.2-2). Additional information: Sect. 6.6.6, Ref. [33]; Sect. 6.6, Ref. [32]; Ref. [35].

Table 3.2-2. Comparison of Stepwise Regression Analyses with Raw and Rank-Transformed Data for Variable *BRAALIC* in Fig. 4b (Table 8.8, Ref. [34]).

Step ^a	Raw Data			Rank-Transformed Data		
	Variable ^b	SRC ^c	R^{2d}	Variable ^b	SRRC ^e	R^{2d}
1	<i>ANHPRM</i>	0.562	0.320	<i>WMICDFL</i> <i>G</i>	-0.656	0.425
2	<i>WMICDFL</i> <i>G</i>	-0.309	0.423	<i>ANHPRM</i>	0.593	0.766
3	<i>WGRCOR</i>	-0.164	0.449	<i>HALPOR</i>	-0.155	0.802
4	<i>WASTWICK</i>	-0.145	0.471	<i>WGRCOR</i>	-0.152	0.824
5	<i>ANHBCEX</i> <i>P</i>	-0.120	0.486	<i>HALPRM</i>	0.143	0.845
6	<i>HALPOR</i>	-0.101	0.496	<i>SALPRES</i>	0.120	0.860
7				<i>WASTWICK</i>	-0.010	0.869

^a Steps in stepwise regression analysis.
^b Variables listed in order of selection in regression analysis.
^c SRCs for variables in final regression model.
^d Cumulative R^2 value with entry of each variable into regression model.
^e SRRCs for variables in final regression model.

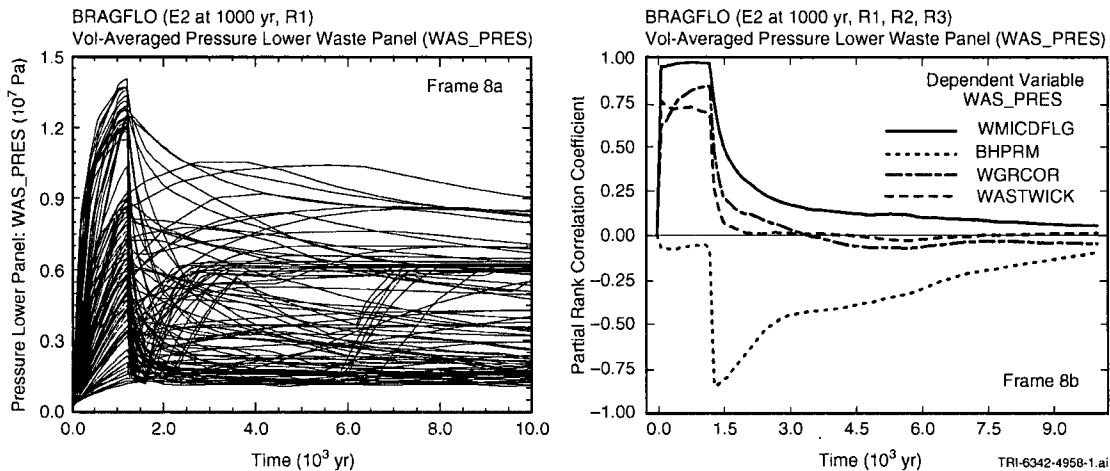


Fig. 3.2.3. Illustration of failure of a sensitivity analysis based on rank-transformed data: (a) Pressures as a function of time and (b) PRCCs as a function of time (Fig. 8.7, Ref. [34]).

For SOARCA the parameter uncertainty and sensitivity analysis will be based upon a mapping between uncertain inputs and analysis results using: 1) Partial rank correlation coefficients (PRCCs); 2) Stepwise rank regression analyses, and 3) Scatter plots.

PRCCs provide a measure of the strength of the monotonic relationships between an independent variable and a dependent variable after a correction has been made to remove the monotonic effects of the other independent variables in the analysis. PRCCs involve the analysis of rank transformed data to transform monotonic relationships into linear relationships. In a stepwise rank regression, the single independent variable that makes the largest contribution to the uncertainty in the dependent variable is selected in the first step. This process continues until no additional variables are found that make identifiable (i.e., significant) contributions to the uncertainty in the dependent variable. A significance level of 0.01 will be used as the criterion for terminating a stepwise regression analysis. In the context of stepwise regression analysis, variable importance is indicated by (i) order of selection in the stepwise selection process, (ii) incremental changes in cumulative R² values, and (iii) the sign and size of the standardized regression coefficients, (i.e., standardized rank regression coefficients (SRRCs), when rank regression is being used) in the final regression model. Results will be presented as a set of CCDFs. The 25-75% bounds on the CCDF results will be calculated using the bootstrap method. A calculation of the confidence bounds on the mean values for the CCDF and other result metrics (e.g., Fraction of the Cesium released to the environment) will be included.



Section 4.0 Uncertain Parameters and Distributions

The scope and schedule of this uncertainty analysis do not allow for a detailed technical basis to be developed for what parameters to include as uncertain inputs or their distributions. Instead, the uncertain parameters and their distributions were identified/characterized by an informal elicitation of subject matter experts. The subject matter experts were asked define distributions for the parameters which they considered most important. They were also asked to provide a technical basis for the distribution definitions. For some uncertain parameters the subject matter experts were able to provide a documented technical basis, however, other uncertain parameters currently have a limited to no documented technical basis. This issue of technical basis documentation will be resolved in the report that documents the overall uncertainty analysis. The results of the elicitation are contained in Sections 4.1 and 4.2 for the MELCOR and MACCS2 parameters, respectively.

4.1 MELCOR Parameters and Distributions

The MELCOR uncertain parameters are divided to cover the following issues:

- sequence issues
- in-vessel accident progression issues
- ex-vessel accident progression issues
- containment behavior issues
- fission product release, transport, and deposition

Uncertainty in Lambda in SRV stochastic failure to reclose: NUREG/CR-6928 describes an analysis of industry-average experience for this event. The recommended distribution is described in NUREG/CR-6928, Table 5-1 (SRV FTC -- SRV failure to close) (see Table 4.1-1 and Figure 4.1-1).

Duration of DC power: This parameter is influenced by the efficiency of operator actions to shed non-essential loads and the age of the batteries. The mode is the value used in the deterministic SOARCA analysis (see Table 4.1-1 and Figure 4.1-2).

Table 4.1-1. MELCOR Uncertain Parameters – Sequences Issues

parameter	distribution
uncertainty in lambda in SRV stochastic failure to reclose	beta distribution mean = 7.95E-04 alpha = 0.5 beta = 6.281E+02 error factor = 8.4
duration of dc power	triangle distribution LB = 2.0 hr mode = 4.0 hr UB = 8.0 hr

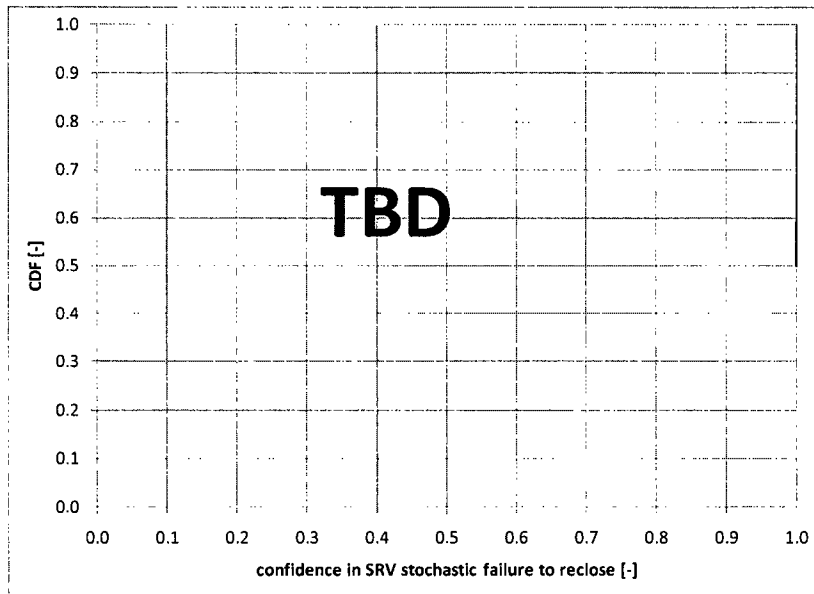


Fig. 4.1-1. CDF of Confidence in SRV Stochastic Failure to Close.

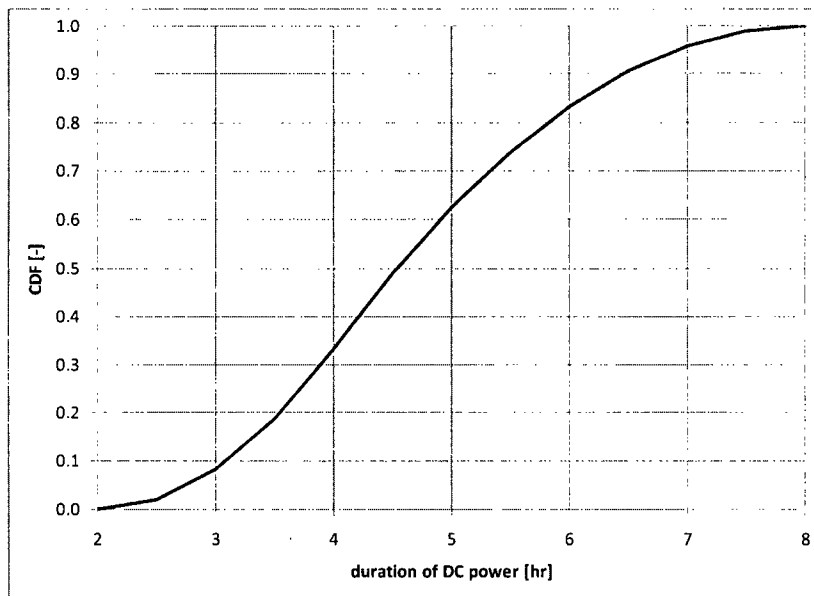


Fig. 4.1-2. CDF of Duration of DC Power.



Zr melt breakout temperature: This parameter represents a collection of uncertain properties that determine the conditions at which oxidized clad mechanically fails, releasing molten unoxidized Zr. This initiates the downward drainage of molten Zr on a ring-by-ring basis in MELCOR. Observed to be among the more important uncertain parameters in prior work on in-vessel melt progression (H2 uncertainty study). The lower bound value is the Zr melt temperature; the upper bound value is based on likely rod collapse temperature. The mode is the value used in the deterministic SOARCA analysis (see Table 4.1-2 and Figure 4.1-3).

Molten clad drainage rate: Time constant for heat transfer to substrate vs downward flow. Another key parameter in the H2 uncertainty study. This parameter represents effective downward flow rate, balancing heat transfer and freezing on substrate against vertical momentum. The mode is the value used in the deterministic SOARCA analysis (see Table 4.1-2 and Figure 4.1-4).

Criteria for thermal seizure of SRV due to heating after onset of core damage: Gas exposure time during open cycles, heat conduction within valve and expansion of valve components. The MELCOR model estimates the thermal response of a representative valve internal component (perhaps the valve stem) as a solid steel cylinder, heated by the gas discharged through the valve (when open). The valve is assumed to seize in the open position on the first cycle above a specified component temperature. Uncertainty in valve thermal response, expansion, and seizure is rolled up into the single value of this component temperature. The mode is the value used in the deterministic SOARCA analysis (see Table 4.1-2 and Figure 4.1-5).

SRV open area after thermal seizure: Thermal expansion of valve would occur primarily during periods of gas flow (open cycles), although penetration (conduction) of heat transferred to inner surfaces would occur over a longer period of time (valve open or closed). These uncertainties lead to large uncertainty on valve position immediately prior to seizure and to the final stem position after seizure (see Table 4.1-2 and Figure 4.1-6).

Main steam line creep rupture area: Pre-existing flaws, weld locations, upper RPV and steam line circulation flow patterns, pipe stress, etc. Creep rupture is monitored at two locations (main steam line nozzle and initial length of main steam line piping). The current model preserves the total flow area of the main steam line, but partitions this area between the intact pipe and the rupture opening. Therefore, a rupture open fraction of 1.0 also closes flow through the main steam line; a value of 0.5 partitions the MSL flow equally between the intact pipe flow path and the rupture flow path. Therefore, the creep rupture open fraction is the numerical complement of the main steam line open fraction, which is defined in file 'MSLcreep.gen'. Uncertainty in the parameters affecting the calculated potential for creep is neglected in this assessment because prior experience suggests the L-M damage index transitions from zero to values well above unity within a very short time (see Table 4.1-2 and Figure 4.1-7).

Fuel failure criterion (transformation of intact fuel to particulate debris): MELCOR lacks a deterministic model for evaluating fuel mechanical response to the effects of clad oxidation, material interactions (eutectic formation), Zircaloy melting, fuel swelling and other processes



that occur at very high temperatures. In lieu of detailed models in this area, a simple temperature-based criterion is used to define the threshold beyond which normal ("intact") fuel rod geometry can no longer be maintained, and the core materials at a particular location collapse into particulate debris. The temperature-based criterion rolls up uncertainties in numerous physio-chemical processes that affect fuel rod integrity. The basic idea behind this "time-at-temperature" criterion, however, is that the endurance of the upright, cylindrical configuration of fuel rod bundles decreases with increasing temperature. A temperature-based 'cumulative damage' criterion is used in the MELCOR model to define the remaining lifetime of normal fuel rod geometry. The alternative functions represent shifts in temperature of +/- 100 K and fuel endurance times of +/- factor of 2.0 (see Table 4.1-2, Figure 4.1-8, and Figure 4.1-9).

Radial debris relocation time constants: This specific parameter is used as a surrogate for the broad uncertainty of debris relocation rate into water in the lower head. This, in turn, affects the potential for debris coolability in the lower head (faster relocation rates decrease coolability; slower rates improve coolability). Debris relocation in MELCOR is relatively discrete, and occurs when the lower core plate in a particular ring yields. Molten material and particulate debris in that ring immediately fall into the lower head and is followed by debris from adjacent rings at a rate determined by the 'radial relocation time constant.' Adjustments in this parameter should affect the overall rate at which debris enters the lower head after support plate failure. Morphology and temperature distribution within debris field in the vicinity of lower core plate failure. Configuration of debris 'pour' into lower head (see Table 4.1-2, Figure 4.1-10, and Figure 4.1-11).



Table 4.1-2. MELCOR Uncertain Parameters – In-Vessel Accident Progression Issues

parameter	distribution
Zr melt breakout temperature	triangle distribution LB = 2100 K mode = 2400 K UB = 2550 K
molten clad drainage rate	triangle distribution LB = 0.1 kg/m-s mode = 0.2 kg/m-s UB = 1.0 kg/m-s
criteria for thermal seizure of SRV due to heating after onset of core damage	triangle distribution LB = 800 K mode = 900 K UB = 1200 K
SRV open area fraction after thermal seizure	uniform distribution LB = 0.0 UB = 1.0
main steam line creep rupture area fraction	uniform distribution LB = 0.0 UB = 1.0
fuel failure criterion (transformation of intact fuel to particulate debris)	discrete distribution base line case = 0.8 alternate-1 = 0.1 alternate-2 = 0.1
radial debris relocation time constants – solid debris	triangle distribution LB = 180 s mode = 360 s UB = 720 s
radial debris relocation time constants – molten debris	triangle distribution LB = 30 s mode = 60 s UB = 120 s

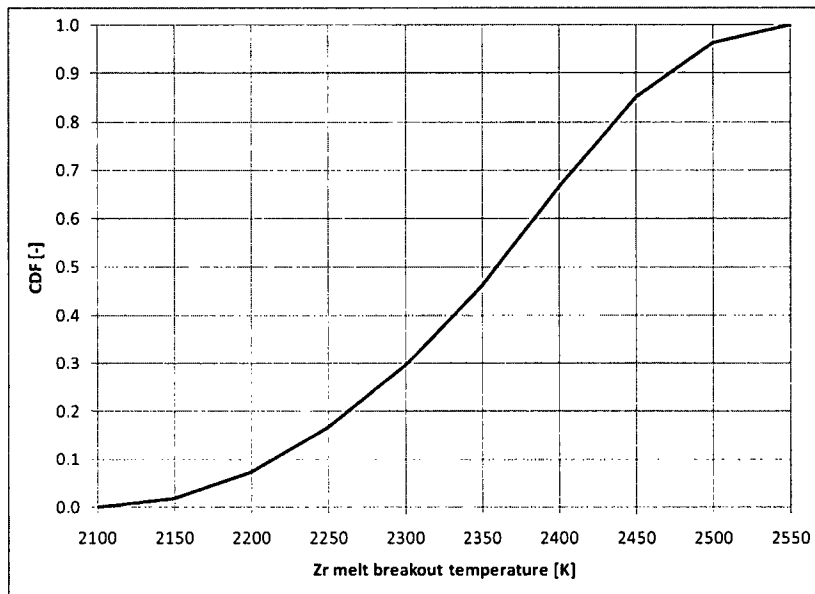


Fig. 4.1-3. CDF of Zr melt breakout temperature.

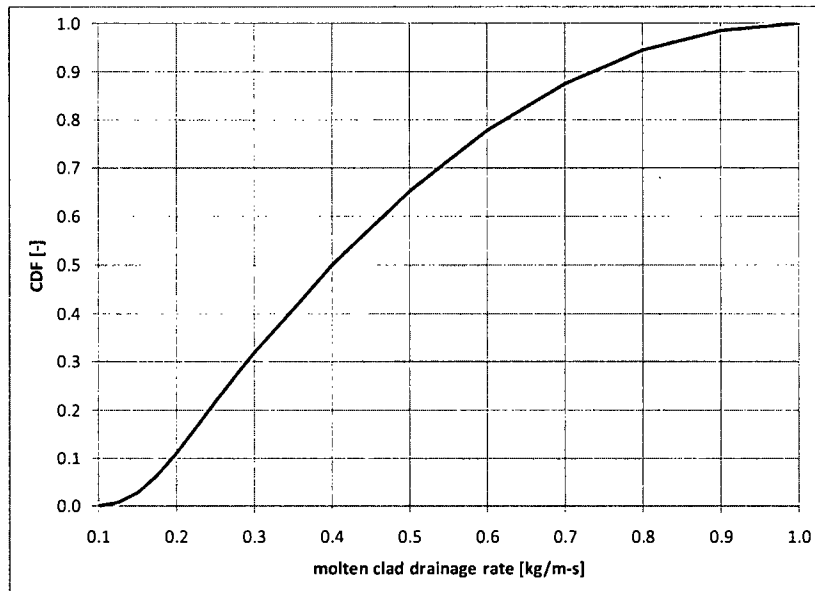


Fig. 4.1-4. CDF of molten clad drainage rate.

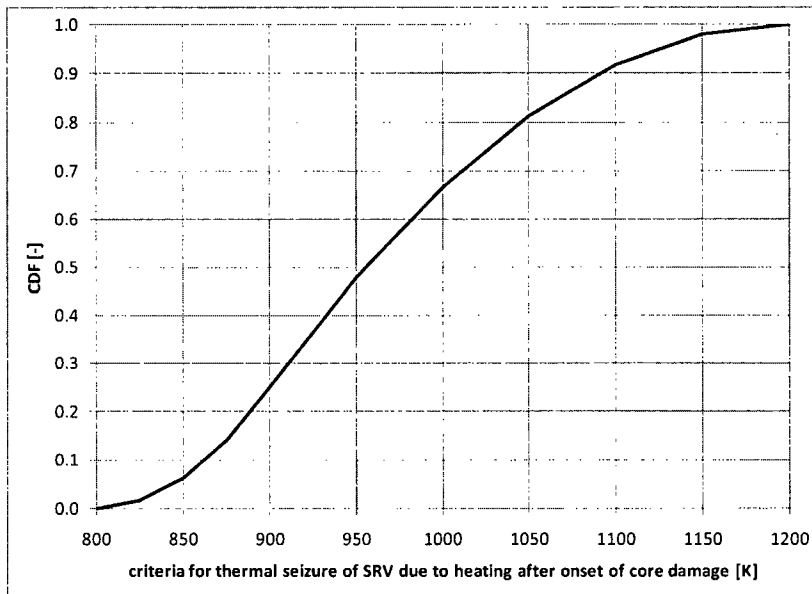


Fig. 4.1-5. CDF of criteria for thermal seizure of SRV due to heating after onset of core damage.

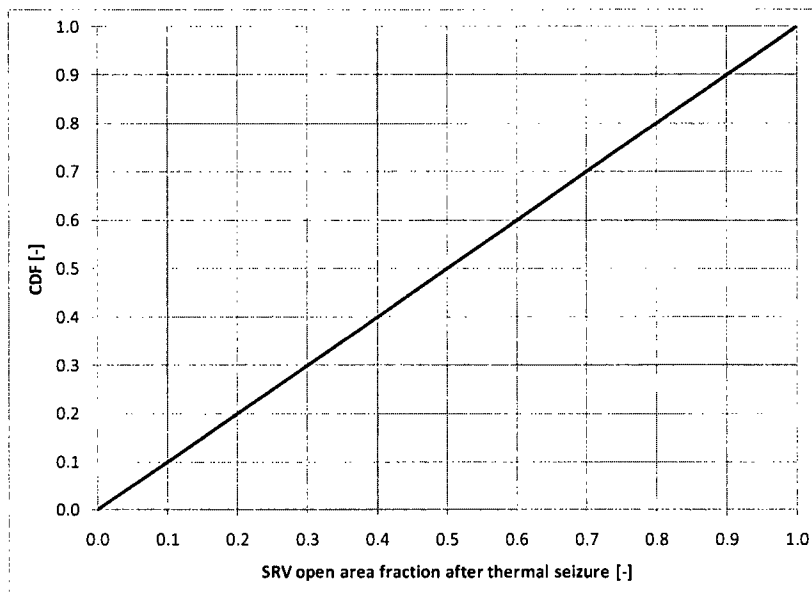


Fig. 4.1-6. CDF of SRV open area fraction after thermal seizure.

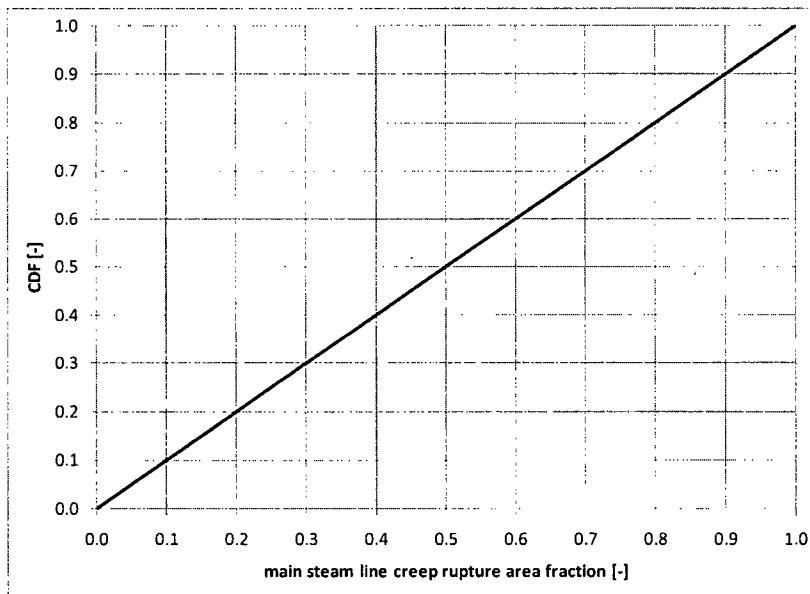


Fig. 4.1-7. CDF of SRV open area fraction after thermal seizure.

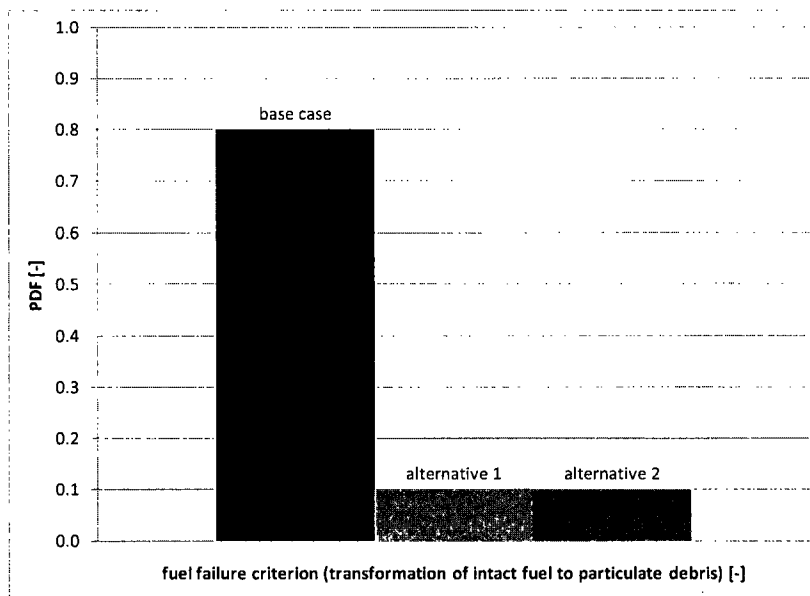


Fig. 4.1-8. PDF of fuel failure criterion (transformation of intact fuel to particulate debris).

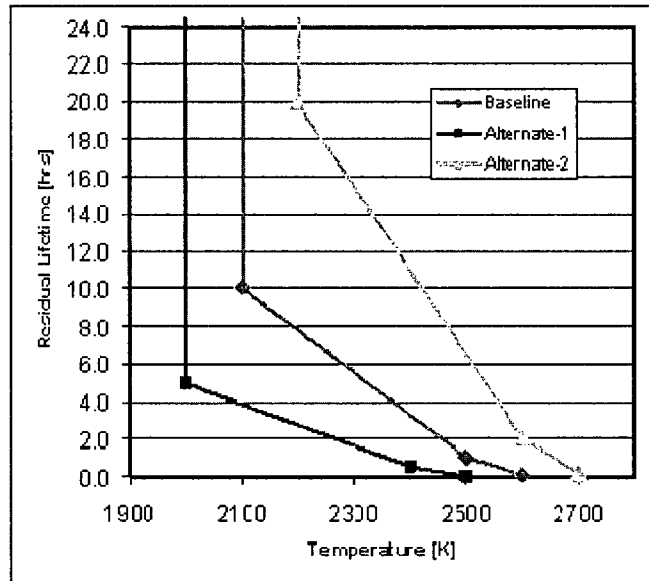


Fig. 4.1-9. Fuel failure criterion functions.

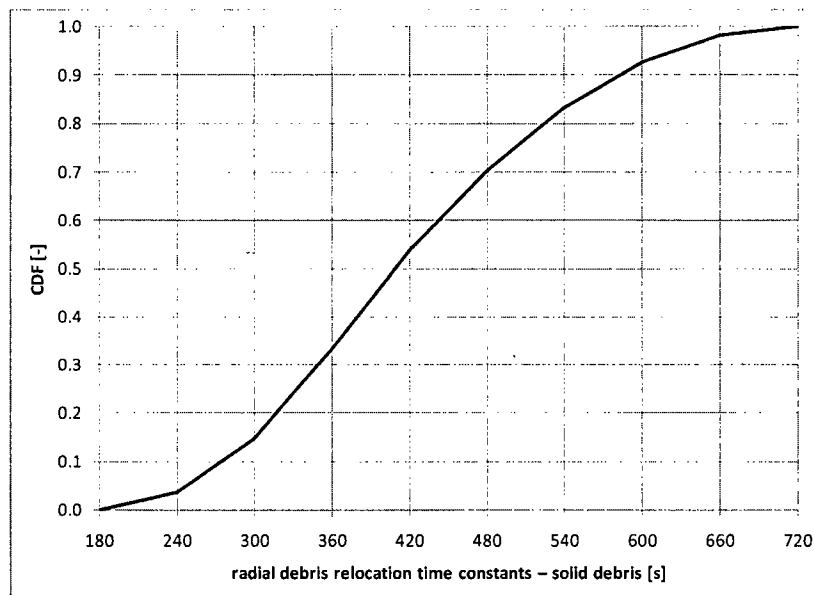


Fig. 4.1-10. CDF of radial debris relocation time constants – solid debris.

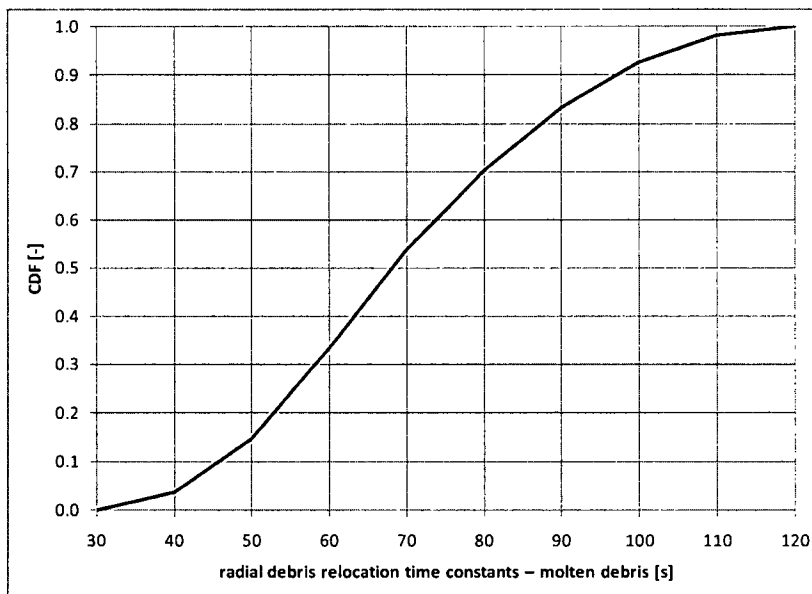


Fig. 4.1-11. CDF of radial debris relocation time constants – liquid debris.



Debris lateral relocation -- cavity spillover criteria and spreading rate: Lateral spread criteria determine whether and when hot debris contact the DW liner. Two principal contributors: (a) Debris (differential) height and temp required for "spill-over" from pedestal to quadrant of DW floor adjacent to pedestal doorway. (b) Debris velocity as it flows across DW floor (from pedestal doorway to liner). This is calculated by CFs assuming a minimum transit time from pedestal to DW liner of 10 min if $T(\text{debris}) > \text{liquidus}$. Velocity is zero when $T(\text{debris}) < \text{solidus}$. Linear interpolation between. Assume max velocity is fixed and base uncertainty on debris temperature for mobility (liquidus). It is assumed lateral debris mobility (spill over from the pedestal to the DW floor) is a function of debris temperature and the differential head (depth) of debris inside versus outside the pedestal doorway. For simplicity, assume the temperatures at which debris begins to move and the value at which its lateral velocity is a maximum are fixed at the values used in the baseline model (i.e., the solidus and liquidus, respectively). Reflect uncertainty in debris mobility by uncertainty in the height of debris (at those temperatures) necessary for lateral movement (see Table 4.1-3, Figure 4.1-12, and Figure 4.1-13).

Table 4.1-3. MELCOR Uncertain Parameters – Ex-Vessel Accident Progression Issues

parameter	distribution
debris overflow head as a function of debris temperature -- T-solidus/no-flow head at 1420 K	uniform distribution LB = 0.5 m UB = 5.0 m
debris overflow head as a function of debris temperature -- T-liquidus at 1670 K	uniform distribution LB = 0.05 m UB = 0.25 m

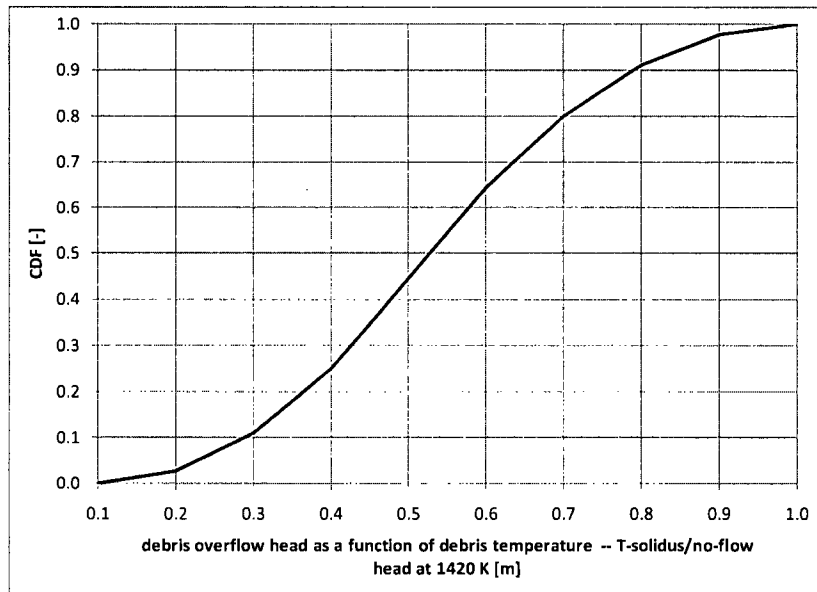


Fig. 4.1-12. CDF debris overflow head as a function of debris temperature -- T-solidus/no-flow head at 1420 K.

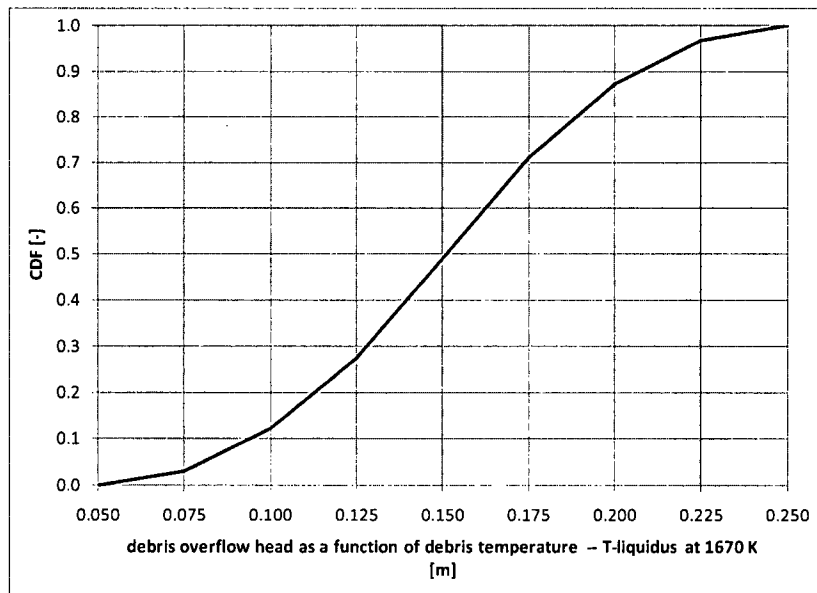


Fig. 4.1-13. CDF of debris overflow head as a function of debris temperature -- T-liquidus at 1670 K.



Flow area resulting from DW liner failure: Failure area affects DW atmosphere discharge rate to reactor building (or post-failure 'residence time.'). Debris temperature, depth against liner and possibility of debris plugging part of opening in liner (see Table 4.1-4 and Figure 4.1-14).

Hydrogen ignition criteria (where flammable): No consideration currently given to possibility of the absence of an ignition source in the reactor building. Ignition source for combustion in reactor building unclear during SBO. Default ignition parameters used in baseline calculations. Accumulation of H₂ due to absence of ignition source is credible (see Table 4.1-4 and Figure 4.1-15).

Railroad door open fraction due to over-pressure failure in reactor building: The mechanical response of the large doors at both ends of the equipment tunnel into the reactor building affects air infiltration and the establishment of a "chimney effect" through the building. This, in turn, greatly reduces the aerosol residence time and the building DF. Smaller open areas are credible and might reduce the airflow and increase residence time. The large equipment access doors on the 135-ft level of the RB area assumed to be relatively weak when subjected to large internal pressure loads. Failure by buckling seems rather certain during a modest to strong hydrogen burn. However, the open area that results from failure isn't clear (see Table 4.1-4, Figure 4.1-16, and Figure 4.1-17).

Table 4.1-4. MELCOR Uncertain Parameters – Containment Behavior Issues

parameter	distribution
flow area resulting from DW liner failure	uniform distribution LB = 0.05 m ² UB = 1.0 m ²
hydrogen ignition criteria (where flammable)	triangle distribution LB = 0.04 mode = 0.10 UB = 0.20
railroad door open fraction due to over-pressure failure in RB –inner door	uniform distribution LB = 0.05 UB = 0.75
railroad door open fraction due to over-pressure failure in RB –outer door	uniform distribution LB = 0.05 UB = 0.75

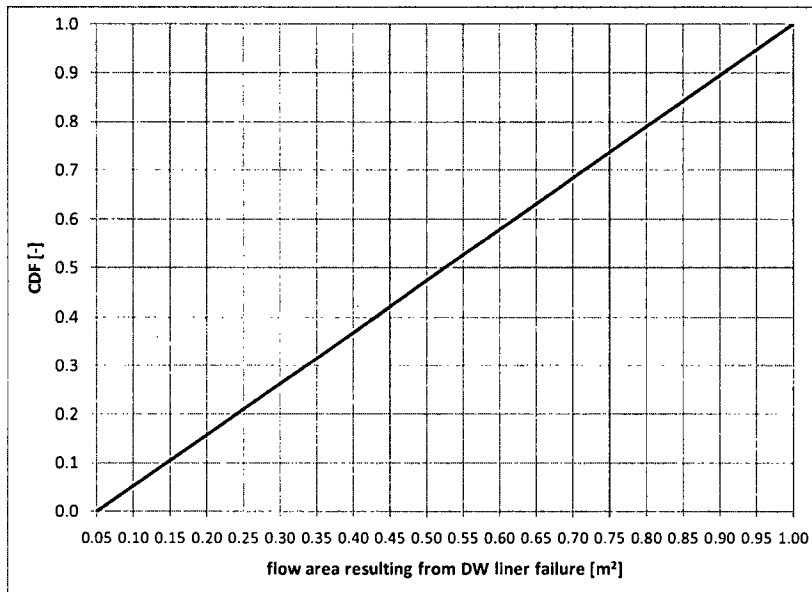


Fig. 4.1-14. CDF of flow area resulting from DW liner failure.

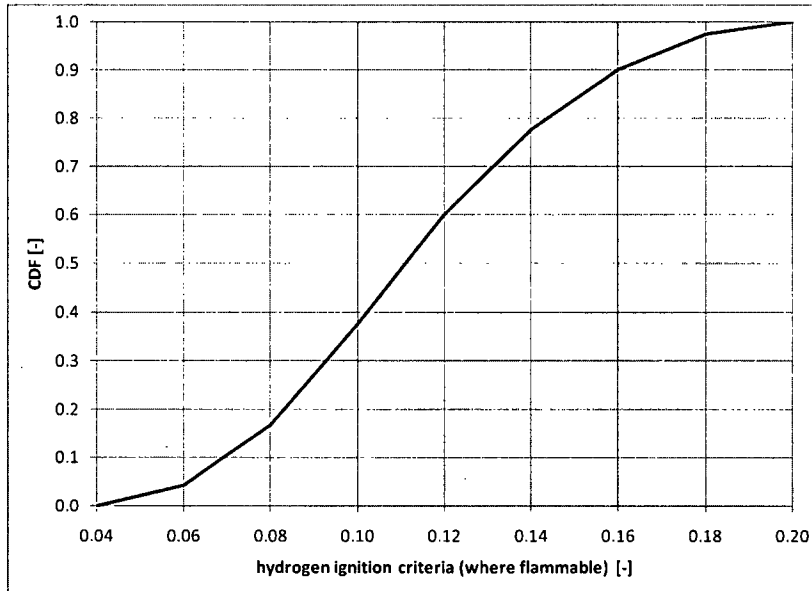


Fig. 4.1-15. CDF of hydrogen ignition criteria (where flammable).

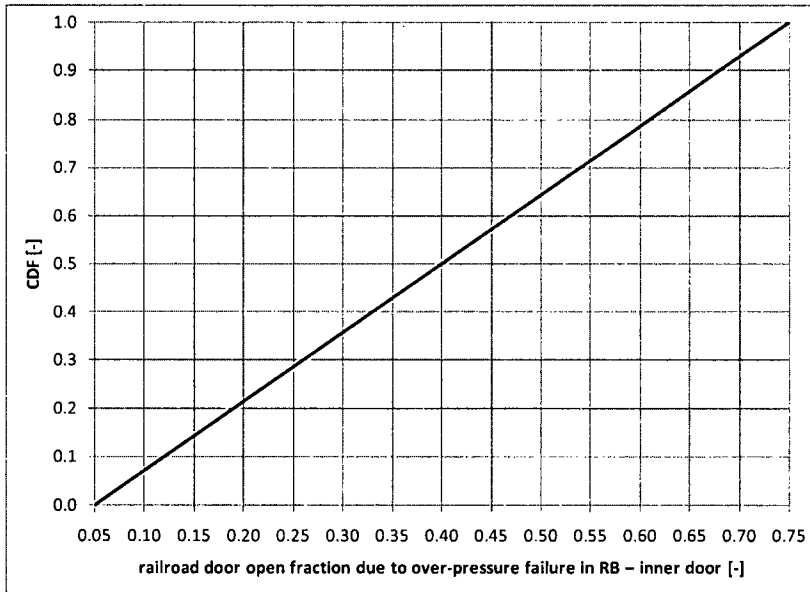


Fig. 4.1-16. CDF of railroad door open fraction due to over-pressure failure in RB – inner door.

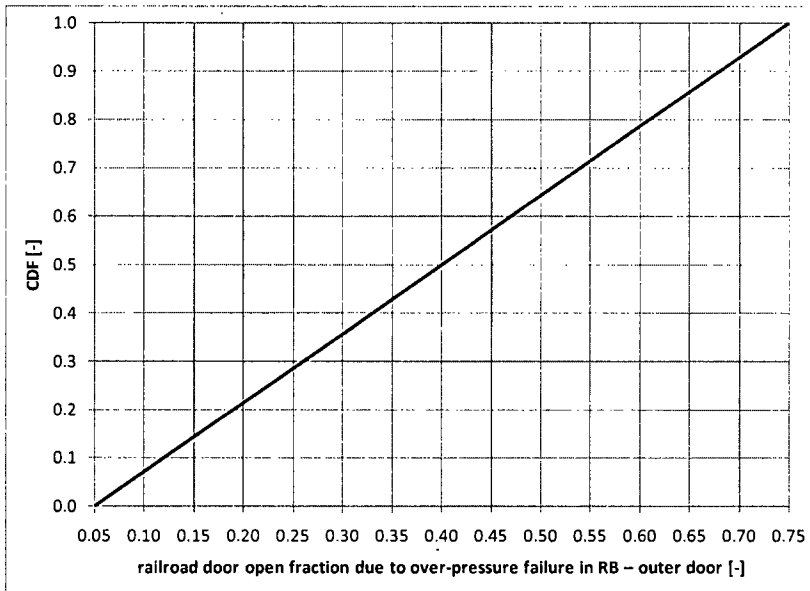


Fig. 4.1-17. CDF of railroad door open fraction due to over-pressure failure in RB – outer door.



Chemical forms of iodine and cesium (I_2 , CH_3I , CsI , $CsOH$, Cs_2MoO_4): Partitioning the initial core inventory of cesium and iodine among certain allowable chemical forms (for release and transport) is managed within a spreadsheet that generates MELCOR input files that define the initial spatial mass distribution of each chemical species and its associated decay heat. Changes to the mass fractions assumed for a particular chemical group directly affect the mass fractions of other chemical groups, and hundreds of individual input records within the MELCOR model for Peach Bottom. Due to the complexity of this general modeling uncertainty, a few alternative sets of MELCOR input files are recommended to span the range of plausible combinations of chemical forms of key radionuclide groups. Fixed partition fractions, preserving mass balances. The physical properties of methyl iodide are not currently defined for an RN class. Therefore, input for a new class (and associated mass balance arithmetic in the core inventory spreadsheets) would be necessary to model this form of iodine. This was considered beyond the scope of this study and CH_3I is neglected. Note: physical properties of $CsOH$ have been replaced by those for Cs_2MoO_4 for RN Class 2 in the standard (DEFAULT 2.0) input. New input must be generated to return RN Class 2 properties to those for $CsOH$ to properly implement this uncertainty issue. One of five alternative combinations of four chemical groups are defined with an associated relative probability (see Table 4.1-5 and Figure 4.1-18).

Table 4.1-5. MELCOR Uncertain Parameters – Chemical Forms of Iodine and Cesium

parameter		distribution			
five alternative combinations of RN classes 2, 4, 16, and 17 (I_2 , CsI , $CsOH$, Cs_2MoO_4)		discrete distribution combination #1 = 0.5 combination #2 = 0.125 combination #3 = 0.125 combination #4 = 0.125 combination #5 = 0.125			
		$CsOH$	I_2	CsI	Cs_2MoO_4
combination #1	fraction iodine	--	0.0	1.0	--
	fraction cesium ⁵	0.0	--	--	1.0
combination #2	fraction iodine	--	0.0	1.0	--
	fraction cesium	0.50	--	--	0.50
combination #3	fraction iodine	--	0.05	0.95	--
	fraction cesium	0.0	--	--	1.0
combination #4	fraction iodine	--	0.05	0.95	--
	fraction cesium	0.50	--	--	0.50
combination #5	fraction iodine	--	0.02	0.98	--
	fraction cesium	1.0	--	--	0.0

⁵ This represents the distribution of 'residual' cesium -- that is, the mass of cesium remaining after first reacting with the amount of iodine assumed to form CsI .

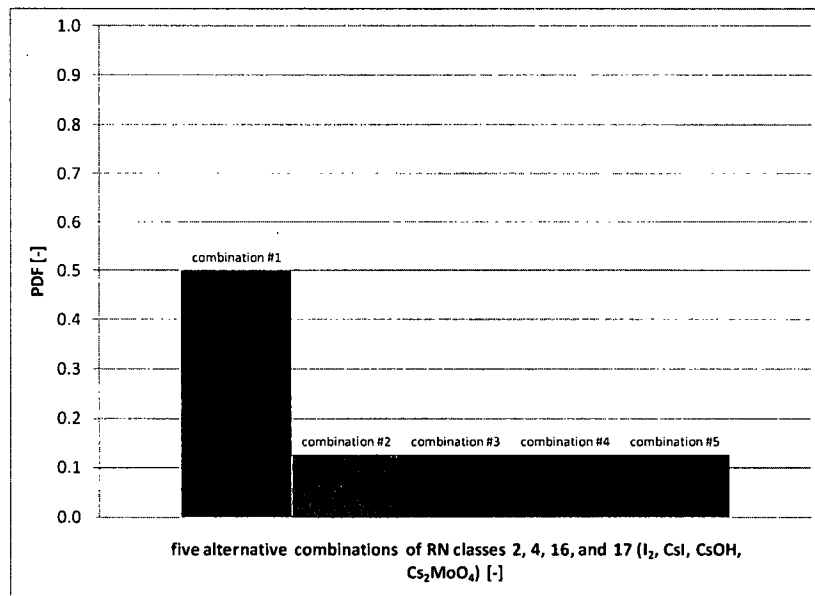


Fig. 4.1-18. CDF of five alternative combinations of RN classes 2, 4, 16, and 17 (I₂, CsI, CsOH, Cs₂MoO₄).



Aerosol deposition physics -- Dynamic and Agglomeration Shape Factors: The particular selection of P and Q (p=1, q=3) produces a distribution that is biased towards 1.0, with diminishing likelihood for Chi and Gamma as the limit of 5 is approached. This specification expresses the belief that the shape factor lies closer to the range of 1 to 3 with diminishing likelihood of having values approaching 5. The lower bound of 1.0 represents perfectly spherical aerosol particles and the upper bound of 5 represents chains of particles. It is rationalized that hygroscopic effects will induce some condensation of moisture on the particles causing the particles to tend towards being spherical and limiting the degree of non-spherical shape (see Table 4.1-6 and Figure 4.1-19).

Aerosol deposition physics -- Particle Density: Material density for the aerosol particles is taken as uncertain within the range of 1000 to 5000 kg/m³ with a bias around 2000 kg/m³ based on the fact that the aerosol can become wet and the particle agglomerates not fully dense with respect to their apparent spherical size. A density of 5000 kg/m³ would be representative of 50% dense agglomerates of UO₂ (see Table 4.1-6 and Figure 4.1-20).

Table 4.1-6. MELCOR Uncertain Parameters – Aerosol Deposition.

parameter	distribution
Dynamic and Agglomeration Shape Factors	beta distribution LB = 1.0 UB = 5.0 alpha = 1.0 beta = 3.0
Particle Density	beta distribution LB = 1000 kg/m ³ UB = 5000 kg/m ³ alpha = 2.0 beta = 2.5

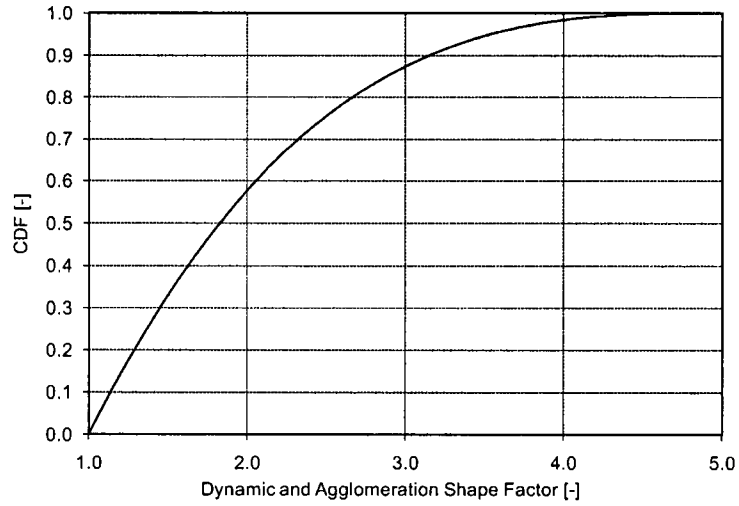


Fig. 4.1-19. CDF of dynamic and agglomeration shape factors.

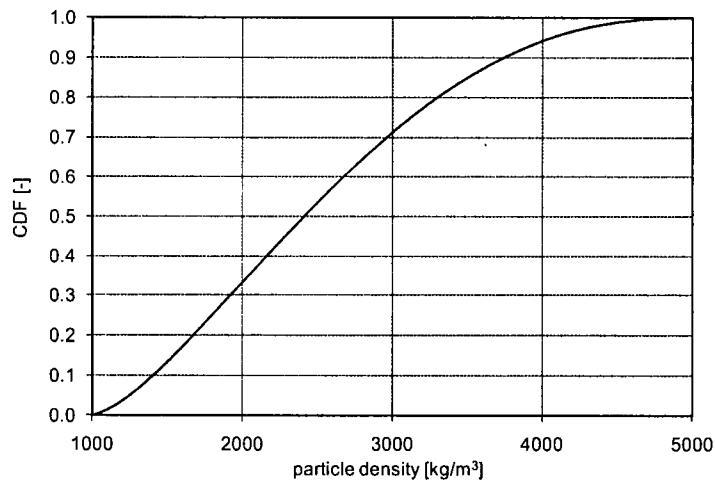


Fig. 4.1-20. CDF of particle density.



4.2 MACCS2 Parameters and Distributions

Documentation of for the technical basis of the uncertain parameters for MACCS2 was provided by the subject matter experts, based upon NUREG/CR⁶ “*Evaluation of Distributions Representing Important Non-Site-Specific Parameters in Off-Site Consequence Analyses*”. This document has not been assigned a NUREG number yet, as such, only the parameters and their definitions are currently provided. This lack of documentation will be resolved in the final report that documents the overall uncertainty analysis. The parameters used in this analysis are given in Tables 4.2-1 through 4.2-10 and in Figures 4.2-1 through 4.2-15.

⁶ This document presents ranges of values and degrees of belief for non-site specific parameters that are uncertain in health consequence analyses related to accidental release of nuclear material, based on a series of expert elicitations conducted in the past by the United States and the Commission of European Communities.



Table 4.2-1. MACCS2 Uncertain Parameters – Washout Model

Linear Coefficient in Washout Model	Percentile	CWASH1 [1/s]
continuous logarithmic distribution	0	2.73E-08
	1	2.92E-07
	5	9.13E-07
	10	1.73E-06
	25	5.36E-06
	50	1.89E-05
	75	9.84E-05
	90	2.59E-04
	95	5.79E-04
	99	3.78E-03
	100	1.14E-02

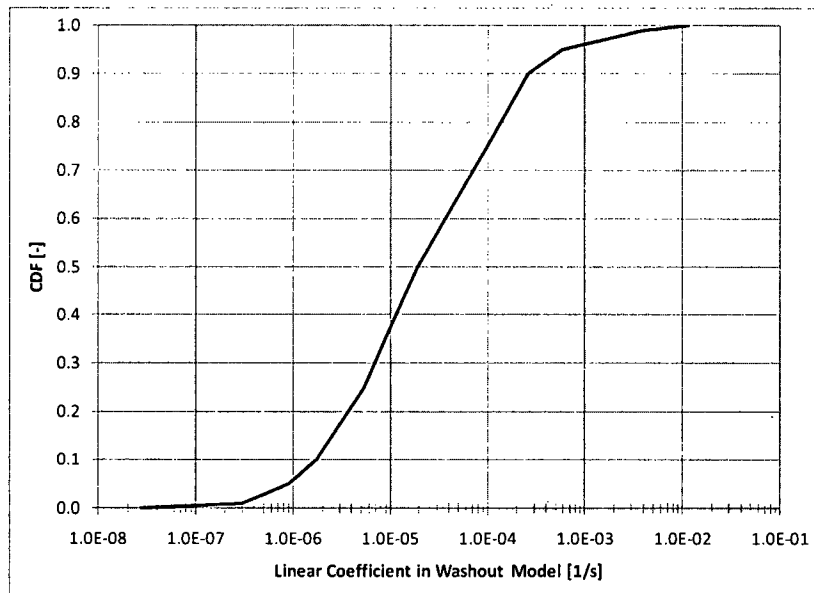


Fig. 4.2-1. CDF of linear coefficient in the washout model.



Table 4.2-2. MACCS2 Uncertain Parameters – Dry Deposition Velocities

Dry Deposition Velocities VDEPOS [m/s] Continuous Logarithmic Distribution																				
Aerosol Bin/Aerosol Median Diameter (micron)																				
Percentile	1	0.12	2	0.21	3	0.40	4	0.74	5	1.38	6	2.57	7	4.79	8	8.91	9	16.59	10	20.00
0	4.44E-07	1.52E-06	4.71E-06	1.34E-05	3.56E-05	9.11E-05	2.28E-04	5.73E-04	1.47E-03	1.96E-03										
1	6.25E-06	7.00E-06	1.10E-05	2.27E-05	5.57E-05	1.51E-04	4.18E-04	1.08E-03	2.42E-03	2.96E-03										
5	5.20E-05	3.99E-05	4.52E-05	7.05E-05	1.42E-04	3.42E-04	9.25E-04	2.62E-03	7.22E-03	9.66E-03										
10	9.60E-05	7.30E-05	7.99E-05	1.19E-04	2.26E-04	5.19E-04	1.35E-03	3.76E-03	1.05E-02	1.42E-02										
25	2.51E-04	1.86E-04	2.00E-04	2.92E-04	5.38E-04	1.16E-03	2.75E-03	6.59E-03	1.49E-02	1.87E-02										
50	8.80E-04	6.63E-04	7.47E-04	1.14E-03	2.10E-03	4.26E-03	8.56E-03	1.53E-02	2.21E-02	2.33E-02										
75	3.13E-03	2.48E-03	2.69E-03	3.76E-03	6.36E-03	1.22E-02	2.47E-02	4.98E-02	9.39E-02	1.11E-01										
90	7.35E-03	5.60E-03	6.03E-03	8.67E-03	1.57E-02	3.36E-02	8.03E-02	2.02E-01	5.03E-01	6.55E-01										
95	1.45E-02	1.11E-02	1.21E-02	1.78E-02	3.32E-02	7.42E-02	1.87E-01	5.00E-01	1.34E+00	1.79E+00										
99	4.99E-02	3.92E-02	4.25E-02	6.06E-02	1.09E-01	2.33E-01	5.72E-01	1.53E+00	4.28E+00	5.84E+00										
100	1.11E-01	8.92E-02	1.00E-01	1.48E-01	2.72E-01	5.83E-01	1.37E+00	3.35E+00	7.95E+00	1.02E+01										

Note: VDEPOS is perfectly rank correlated across aerosol sizes.

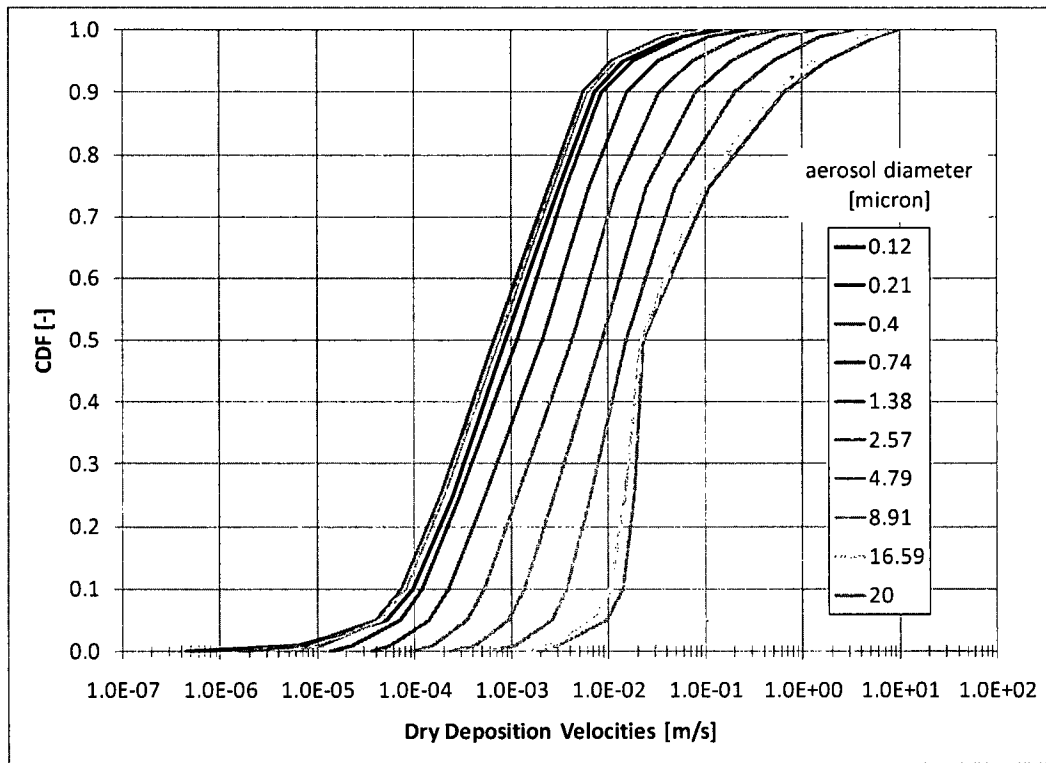


Fig. 4.2-2. CDFs of dry deposition velocities.



Table 4.2-3. MACCS2 Uncertain Parameters – Shielding

	Percentile	Shielding Factors for Evacuation		Shielding Factors for Normal Activity		Shielding Factors for Sheltering		Long-Term Shielding Factors
		Cloudshine [-]	Groundshine [-]	Cloudshine [-]	Groundshine [-]	Cloudshine [-]	Groundshine [-]	Groundshine [-]
Continuous Linear Distribution	0	0.230	0.083	0.600	0.0528	0.500	0.0153	0.0528
	1	0.232	0.128	--	0.0683	--	0.0222	0.0683
	5	0.244	0.182	--	0.0951	--	0.0347	0.0951
	15	0.350	0.243	--	0.129	--	0.0474	0.129
	25	0.457	0.280	--	0.154	--	0.0638	0.154
	50	0.724	0.396	--	0.216	--	0.104	0.216
	75	0.877	0.552	--	0.303	--	0.168	0.303
	85	0.938	0.641	--	0.346	--	0.203	0.346
	95	0.999	0.755	--	0.417	--	0.250	0.417
	99	--	0.870	--	0.489	--	0.288	0.489
100	1.000	0.935	0.950	0.548	0.700	0.331	0.548	

Note: (1) Cloudshine and groundshine shielding factors are correlated for each activity type using a 0.5 rank correlation coefficient.
 (2) These parameters are the best information currently available, however it is known that they will possibly be revised as part of upcoming SOARCA uncertainty analysis.

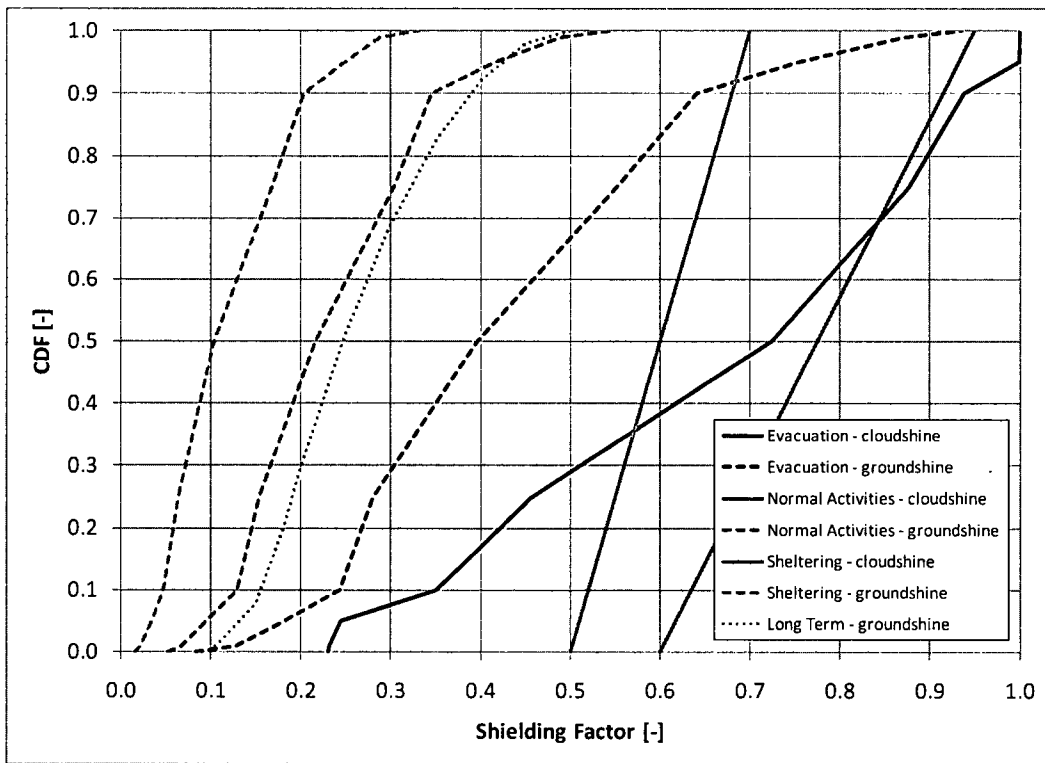


Fig. 4.2-3. CDFs of shielding factors.



Table 4.2-4. MACCS2 Uncertain Parameters – Early Health Effects

Early Health Effects Continuous Linear Distribution												
	Hematopoietic S.			Pulmonary S.			Gastrointestinal S.			Pneumonitis		
Percentile	LD-50 EFFACA [Sv]	Beta EFFACB [-]	Threshold EFFTHR [Sv]	LD-50 EFFACA [Sv]	Beta EFFACB [-]	Threshold EFFTHR [Sv]	LD-50 EFFACA [Sv]	Beta EFFACB [-]	Threshold EFFTHR [Sv]	D-50 EFFACA [Sv]	Beta EFFACB [-]	Threshold EFFTHR [Sv]
0	2.00	2.39	0.667	10.0	3.7	5.3	4.80	3.21	2.000	5.00	3.47	2.67
1	2.41	2.54	0.803	12.0	3.8	6.7	6.18	3.25	2.932	7.30	3.62	3.48
5	3.32	2.83	1.113	16.6	4.4	8.6	7.88	3.41	3.773	8.86	4.04	4.43
10	3.69	3.19	1.316	17.8	4.7	9.6	8.51	3.64	4.499	10.27	4.65	5.05
25	4.38	4.15	1.716	19.9	5.6	11.5	10.02	5.99	5.351	12.90	5.14	6.51
50	5.59	6.07	2.319	23.5	9.6	13.6	12.12	9.31	6.516	16.59	7.34	9.24
75	7.24	10.23	3.560	33.6	13.8	18.4	14.94	11.04	7.671	20.33	14.83	11.34
90	8.89	13.22	4.629	42.0	16.9	22.1	17.65	16.01	8.784	25.75	19.29	14.25
95	10.32	14.28	5.256	45.0	18.7	24.0	19.14	18.03	9.522	31.10	22.06	16.58
99	11.84	15.82	6.188	55.7	21.4	32.4	23.35	19.52	12.962	36.53	65.41	20.74
100	16.50	15.99	8.550	76.5	21.7	37.5	30.00	19.94	15.000	55.50	83.83	28.50

Note: For each health effect, D-50 or LD-50 is correlated with the Threshold using a 0.99 rank correlation coefficient.

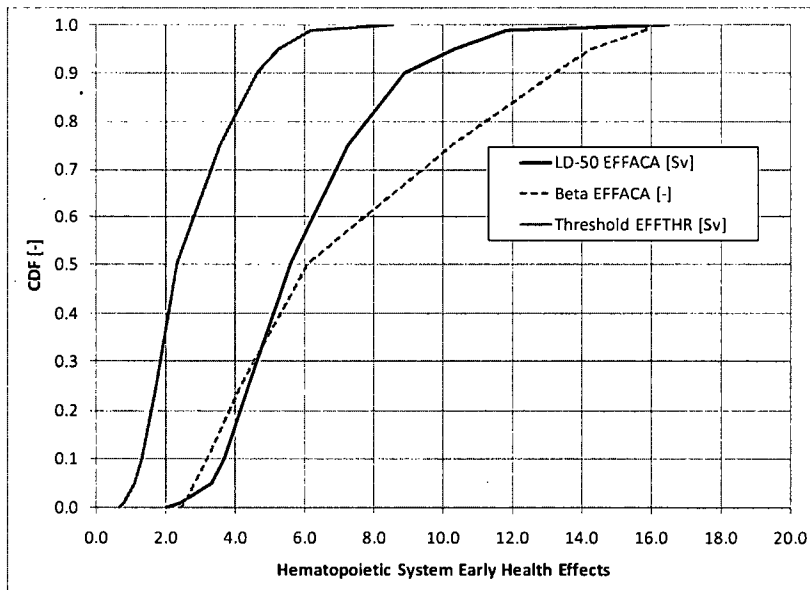


Fig. 4.2-4. CDFs of hematopoietic system early health effects.

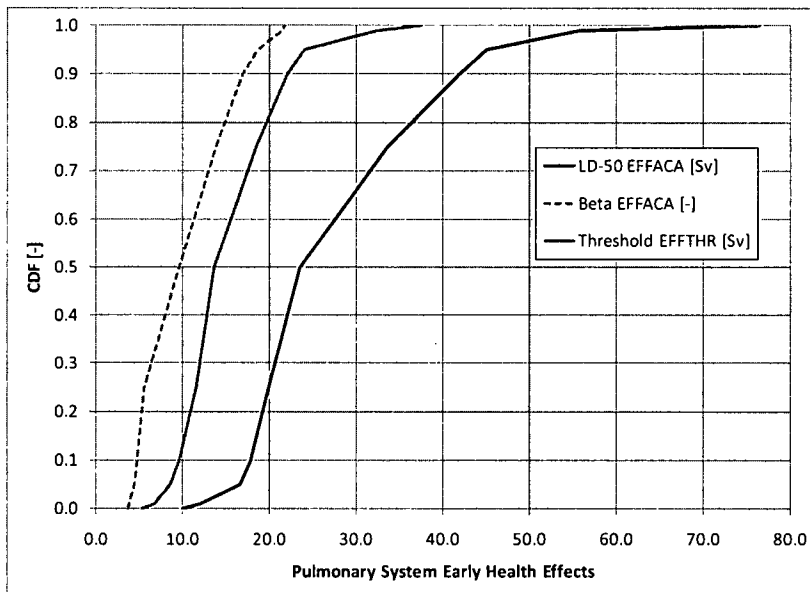


Fig. 4.2-5. CDFs of pulmonary system early health effects.

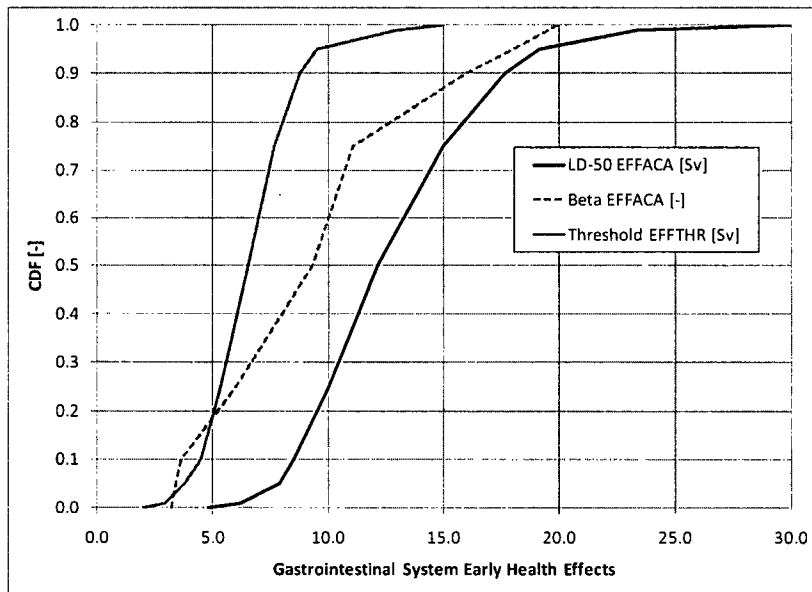


Fig. 4.2-6. CDFs of gastrointestinal system early health effects.

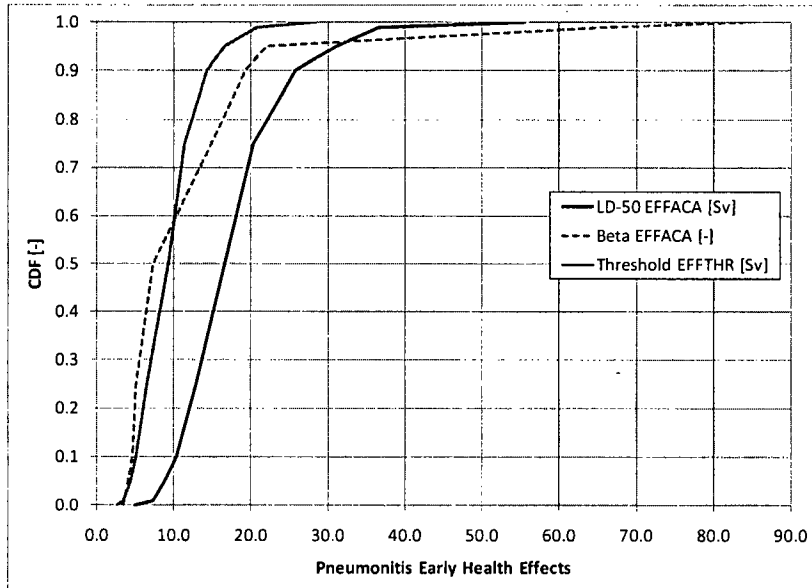


Fig. 4.2-7. CDFs of pneumonitis early health effects.



Table 4.2-5. MACCS2 Uncertain Parameters – Dispersion

Linear, Crosswind Dispersion Coefficients, a(m) (CYSIGA)	Percentile	Stability Class			
		A/B [m]	C [m]	D [m]	E/F [m]
continuous logarithmic distribution	0	0.0650	0.0631	0.0341	0.0212
	1	0.1515	0.0963	0.0562	0.0376
	5	0.2586	0.1564	0.0961	0.0575
	10	0.3381	0.2000	0.1253	0.0768
	25	0.4861	0.2805	0.1845	0.1193
	50	0.7507	0.4063	0.2779	0.2158
	75	1.1379	0.5939	0.4282	0.3730
	90	1.6222	0.8257	0.6080	0.5458
	95	2.0731	0.9735	0.7570	0.6583
	99	3.2179	1.3720	1.1511	0.9467
	100	4.0698	2.0763	1.7618	1.5307
Linear, Vertical Dispersion Coefficients, a(m) (CZSIGA)	Percentile	Stability Class			
		A/B [m]	C [m]	D [m]	E/F [m]
continuous logarithmic distribution	0	0.0056	0.0487	0.0421	0.0533
	1	0.0089	0.0683	0.0752	0.0756
	5	0.0132	0.0871	0.1161	0.1141
	10	0.0166	0.1106	0.1404	0.1310
	25	0.0252	0.1491	0.1821	0.1598
	50	0.0361	0.2036	0.2636	0.2463
	75	0.0598	0.3492	0.4224	0.4617
	90	0.0800	0.5287	0.6048	0.8180
	95	0.0961	0.7039	0.7504	1.1260
	99	0.1336	1.2540	1.4634	2.2051
	100	0.1951	1.8861	3.6880	4.5386
Note: CYSIGA and CZSIGA are perfectly rank correlated with each other and across the stability classes.					

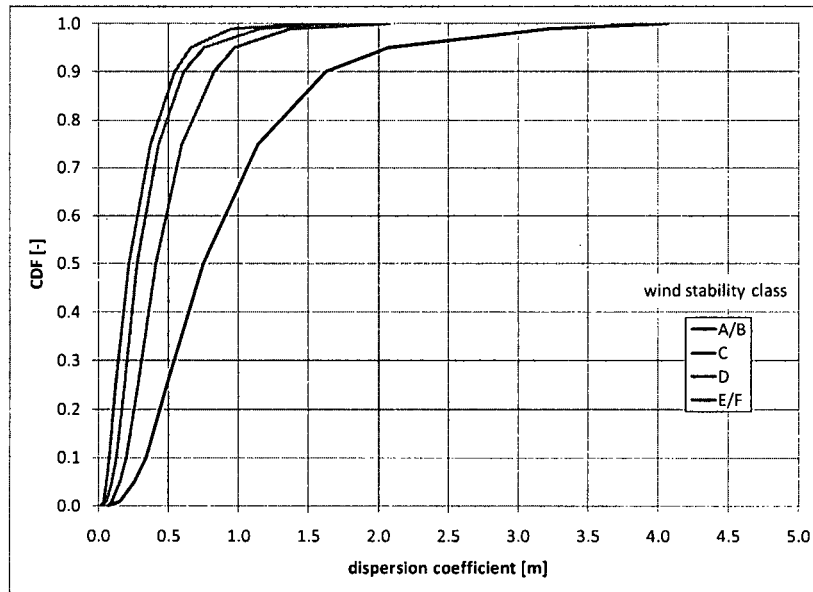


Fig. 4.2-8. CDFs of linear, crosswind dispersion coefficients, a(m).

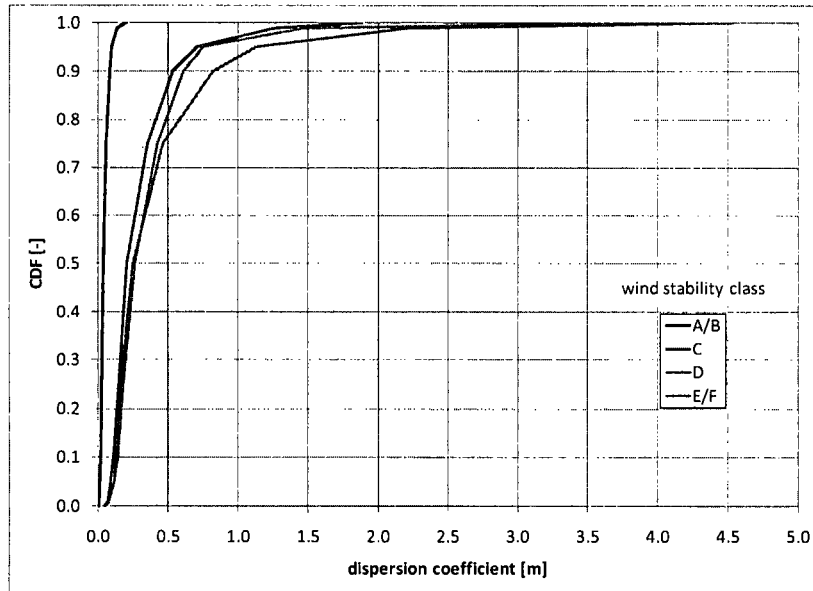


Fig. 4.2-9. CDFs of linear, vertical dispersion coefficients, a(m).



Table 4.2-6. MACCS2 Uncertain Parameters – Habitability

parameter	distribution
long-term phase dose criterion	uniform distribution LB = 1.0 REM UB = 5.0 REM

Note: The long-term dose projection period is set equal to 5.0 yr (1.58E+08 s).

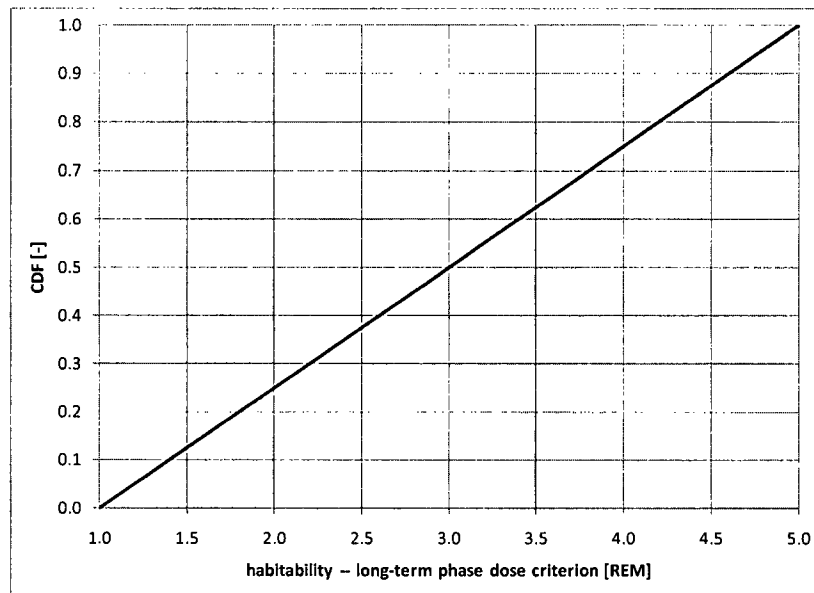


Fig. 4.2-10. CDF of habitability long-term phase dose criterion.



Table 4.2-7. MACCS2 Uncertain Parameters – Relocation Doses and Times

parameter	distribution
hotspot relocation – dose	uniform distribution LB = 1.0 REM UB = 10.0 REM
hotspot relocation – time	uniform distribution LB = 6.0 hr UB = 18 hr
normal relocation – dose	uniform distribution LB = 0.1 REM UB = 1.0 REM
normal relocation – time	uniform distribution LB = 12.0 hr UB = 36.0 hr
Note: Relocation times are perfectly rank correlated. Relocation doses are perfectly rank correlated.	

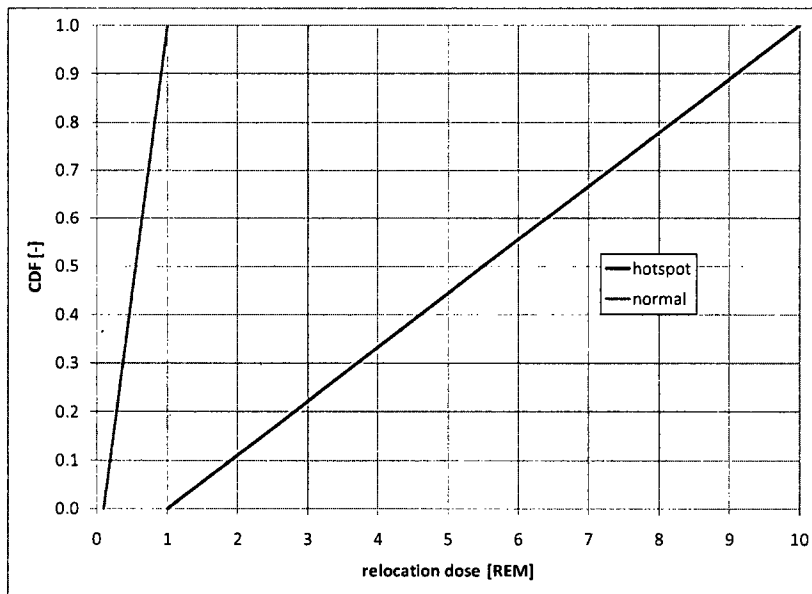


Fig. 4.2-11. CDFs of hotspot and normal relocation doses.

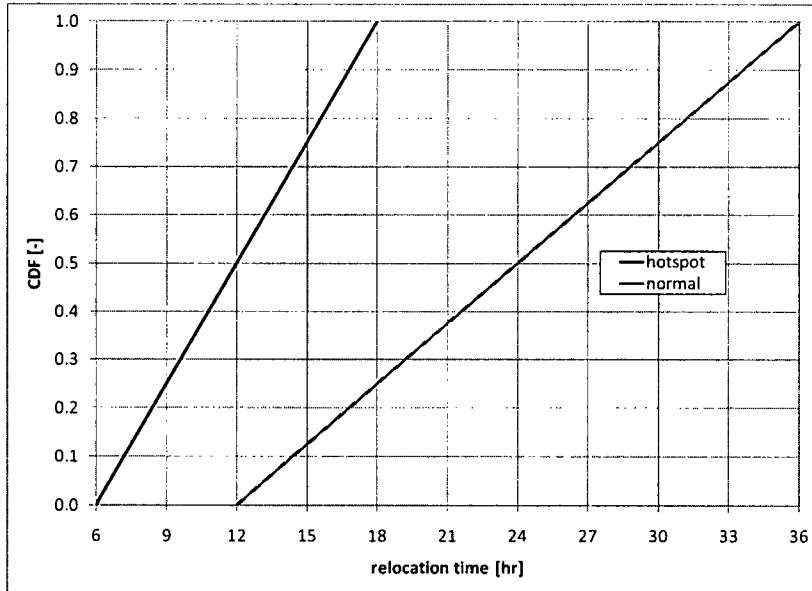


Fig. 4.2-12. CDFs of hotspot and normal relocation times.



Table 4.2-8. MACCS2 Uncertain Parameters – Evacuation Delay

parameter	distribution
evacuation delay – cohort 1	triangle distribution LB = 1.0 hr mode = 2.5 hr UB = 4.0 hr
evacuation delay – cohort 2	triangle distribution LB = 1.0 hr mode = 2.5 hr UB = 4.0 hr
evacuation delay – cohort 3	triangle distribution LB = 1.0 hr mode = 1.0 hr UB = 4.0 hr
evacuation delay – cohort 4	triangle distribution LB = 1.0 hr mode = 5.75 hr UB = 6.0 hr
evacuation delay – cohort 5	triangle distribution LB = 4.0 hr mode = 5.75 hr UB = 8.0 hr

Note: Evacuation delays are sampled independently for each cohort for each radial ring. The evacuation delay is the sum of the delay to shelter and the delay to evacuate.

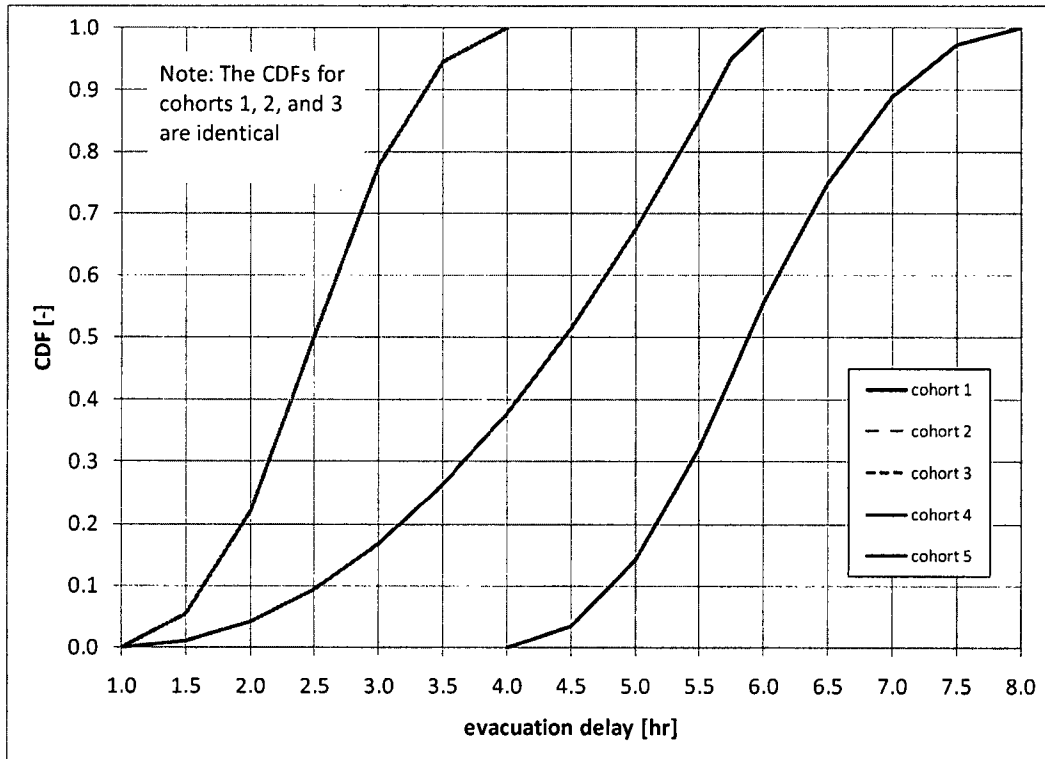


Fig. 4.2-13. CDFs of evacuation delay.



Table 4.2-9. MACCS2 Uncertain Parameters – Evacuation Speed

parameter	distribution
evacuation speed (middle travel phase) – cohort 1	triangle distribution LB = 1.0 mph mode = 3.0 mph UB = 10.0 mph
evacuation speed (middle travel phase) – cohort 2	triangle distribution LB = 1.0 mph mode = 3.0 mph UB = 10.0 mph
evacuation speed (middle travel phase) – cohort 3	uniform distribution LB = 1.0 mph UB = 10.0 mph
evacuation speed (middle travel phase) – cohort 4	uniform distribution LB = 1.0 mph UB = 10.0 mph
evacuation speed (middle travel phase) – cohort 5	uniform distribution LB = 1.0 mph UB = 10.0 mph
Note: Evacuation speeds are perfectly rank correlated between cohorts.	

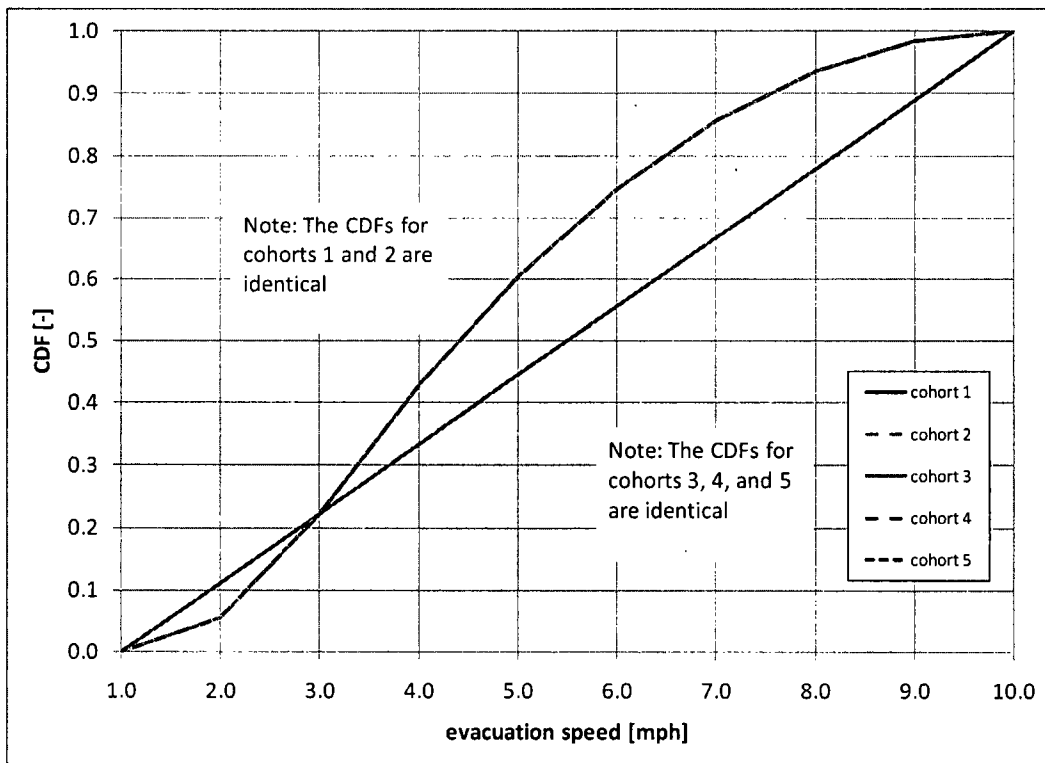


Fig. 4.2-14. CDFs of evacuation speed.



Table 4.2-10. MACCS2 Uncertain Parameters – Dose Threshold

parameter	distribution
dose threshold	uniform distribution LB = 0.0 REM UB = 2.0 REM

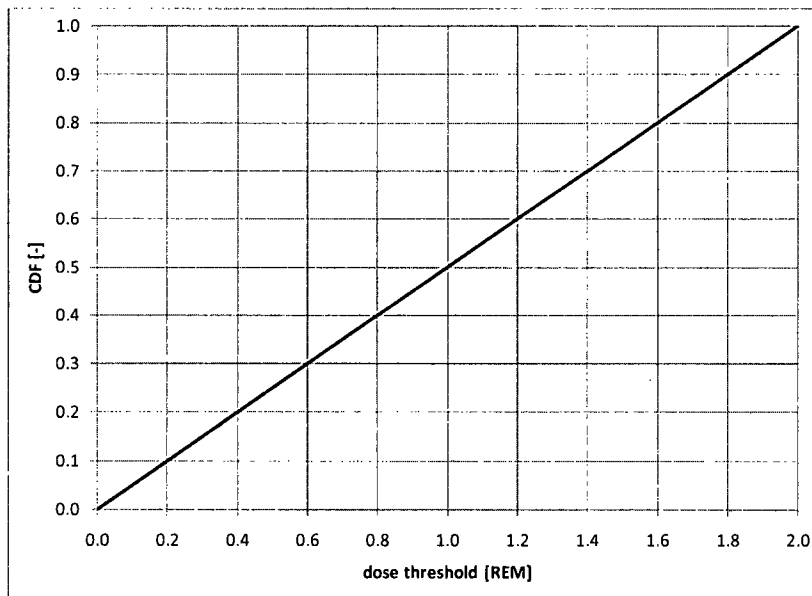


Fig. 4.2-15. CDF of dose threshold.



Section 5.0 Programmatic Constraints and Schedule for Analyses

5.1 Programmatic Constraints

The uncertainty analysis needs to be completed in six months. The NRC desires to have the uncertainty quantification completed when the SOARC NUREG documents goes to public comment in January and the analysis documented in a separate NUREG by the time the SOARCA NUREG is final around June 2011.

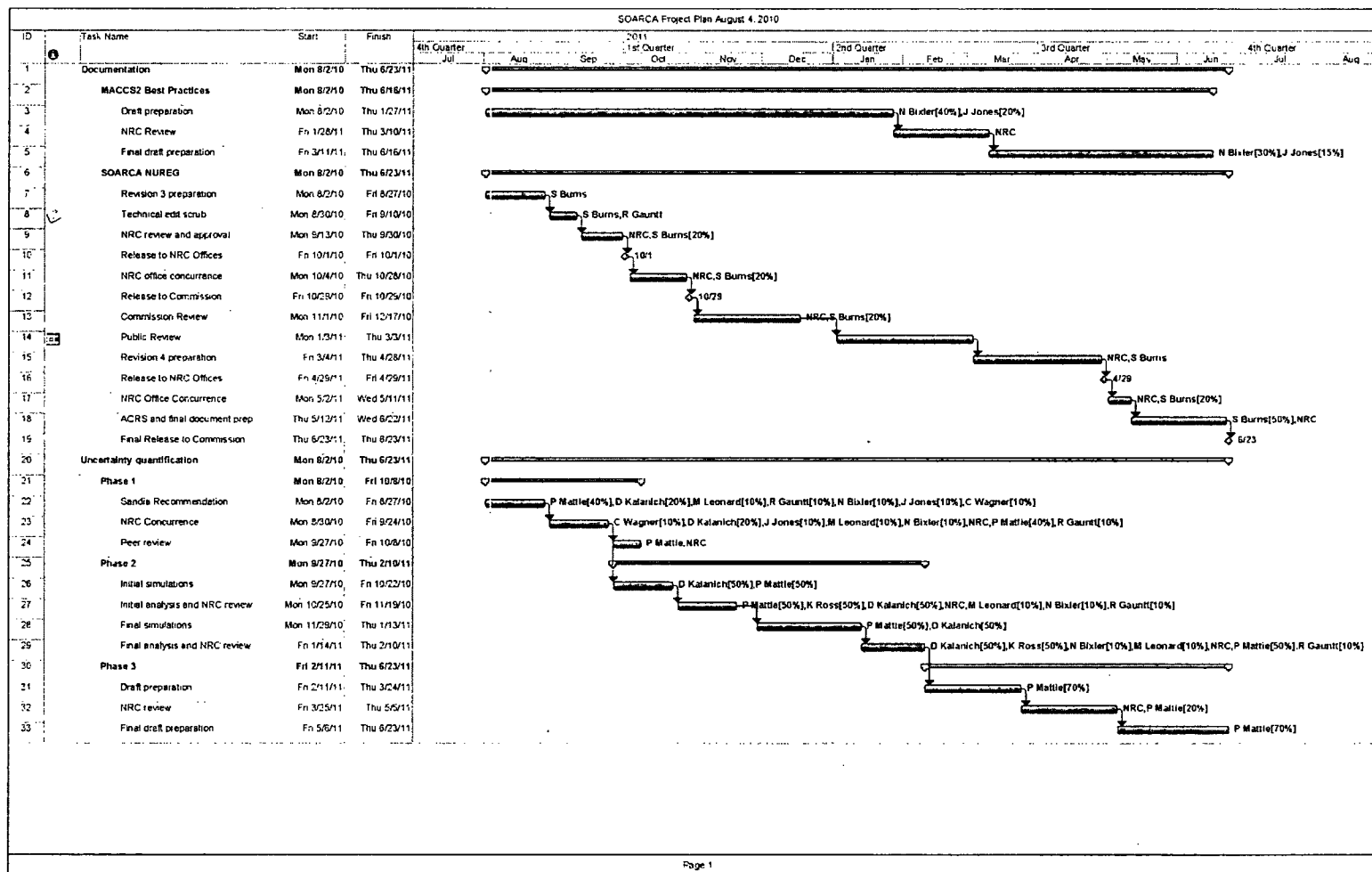
- 1) August 31, 2010, SNL delivered in writing a draft plan for the uncertainty analysis that includes: recommendation of the proposed accident scenario, a description of the recommended approach, and list of parameters and their distributions to be used in the study.
- 2) SNL-NRC continue to evaluate and revise the proposed plan.
- 3) October 26, 2010, Peer review committee meeting on the UA plan
- 4) November 1, 2010, NRC to make final decision on consensus plan.
- 5) Begin the uncertainty analysis November 1, 2010.
- 6) Complete the uncertainty analysis February 28, 2011.

The uncertainty analysis will be used to provide insight as to how uncertainty in a set of important input parameters affect a specific scenario's results, rather than a comprehensive SOARCA uncertainty and sensitivity analysis. The uncertain distributions are highly plant and scenario specific.

- 1) The probabilistic method and uncertainty analysis will utilize the best available software without modification. Currently the best available method utilizes the SNL proposed "inner looping" approach.
- 2) A comprehensive PIRT is not in the work scope, therefore a limited set of parameters and their distributions will be compiled that relies heavily on the best available data and expert judgment.
- 3) The uncertain parameter sensitivity study uses a process which includes several statistical methods, each of which analyze the results to look for monotonic relationships between the uncertain parameters and the distribution of results rather than a comprehensive analysis of each individual probabilistic realization.
- 4) Issues encountered during this analysis will be identified and documented in the final report. A comprehensive analysis of the root cause and iterations (re-running the calculations) will be limited due to schedule constraints.

5.2 Schedule

A draft schedule for completion of the analyses for the SOARCA uncertainty study is attached. (Currently, this draft schedule is delayed by approximately one month.)





Section 6.0 References

1. U.S. NRC (U.S. Nuclear Regulatory Commission). *NRC FORM 189: "State-of-the-Art Reactor Consequence Analyses", DOE Laboratory Cost and Project Proposal for NRC Work, Rev.4, November 18, 2008, Job Code N6306, NRC B&R Number 86015111203, NRC BOC Code 253D, DOE B&R No. 401001060.* Washington, DC: U.S. Nuclear Regulatory Commission 2008.
2. Helton JC. Uncertainty and Sensitivity Analysis in the Presence of Stochastic and Subjective Uncertainty. *Journal of Statistical Computation and Simulation* 1997; 57(1-4):3-76.
3. Helton JC, Burmaster DE. Guest Editorial: Treatment of Aleatory and Epistemic Uncertainty in Performance Assessments for Complex Systems. *Reliability Engineering and System Safety* 1996; 54(2-3):91-94.
4. Paté-Cornell ME. Uncertainties in Risk Analysis: Six Levels of Treatment. *Reliability Engineering and System Safety* 1996; 54(2-3):95-111.
5. Winkler RL. Uncertainty in Probabilistic Risk Assessment. *Reliability Engineering and System Safety* 1996; 54(2-3):127-132.
6. Hofer E. When to Separate Uncertainties and When Not to Separate. *Reliability Engineering and System Safety* 1996; 54(2-3):113-118.
7. Parry GW, Winter PW. Characterization and Evaluation of Uncertainty in Probabilistic Risk Analysis. *Nuclear Safety* 1981; 22(1):28-42.
8. Helton JC. Probability, Conditional Probability and Complementary Cumulative Distribution Functions in Performance Assessment for Radioactive Waste Disposal. *Reliability Engineering and System Safety* 1996; 54(2-3):145-163.
9. Hoffman FO, Hammonds JS. Propagation of Uncertainty in Risk Assessments: The Need to Distinguish Between Uncertainty Due to Lack of Knowledge and Uncertainty Due to Variability. *Risk Analysis* 1994; 14(5):707-712.
10. Helton JC. Treatment of Uncertainty in Performance Assessments for Complex Systems. *Risk Analysis* 1994; 14(4):483-511.
11. Apostolakis G. The Concept of Probability in Safety Assessments of Technological Systems. *Science* 1990; 250(4986):1359-1364.
12. Haan CT. Parametric Uncertainty in Hydrologic Modeling. *Transactions of the ASAE* 1989; 32(1):137-146.
13. Kaplan S, Garrick BJ. On the Quantitative Definition of Risk. *Risk Analysis* 1981; 1(1):11-27.
14. Der Kiureghian A, Ditlevsen O. Aleatory or Epistemic? Does It Matter? *Structural Safety* 2009; 31:105-112.
15. Helton JC. Mathematical and Numerical Approaches in Performance Assessment for Radioactive Waste Disposal: Dealing with Uncertainty. In: EM Scott, ed. *Modelling Radioactivity in the Environment*. New York, NY: Elsevier Science, 2003:353-390.
16. Helton JC, Anderson DR, Jow H-N, Marietta MG, Basabilvazo G. Conceptual Structure of the 1996 Performance Assessment for the Waste Isolation Pilot Plant. *Reliability Engineering and System Safety* 2000; 69(1-3):151-165.



17. Mosleh A, Siu N, Smidts C, Liu C. *Proceedings of Workshop I in Advanced Topics in Risk and Reliability Analysis, Model Uncertainty: Its Characterization and Quantification*. NUREG/CP-0138. Washington, D.C.: U.S. Nuclear Regulatory Commission 1994.
18. Hora SC, Iman RL. Expert Opinion in Risk Analysis: The NUREG-1150 Methodology. *Nuclear Science and Engineering* 1989; 102(4):323-331.
19. Meyer MA, Booker JM. *Eliciting and Analyzing Expert Judgment: A Practical Guide*. New York, NY: Academic Press, 1991.
20. Keeney RL, Winterfeldt DV. Eliciting Probabilities from Experts in Complex Technical Problems. *IEEE Transactions on Engineering Management* 1991; 38(3):191-201.
21. Thorne MC, Williams MMR. A Review of Expert Judgement Techniques with Reference to Nuclear Safety. *Progress in Nuclear Safety* 1992; 27(2-3):83-254.
22. Thorne MC. The Use of Expert Opinion in Formulating Conceptual Models of Underground Disposal Systems and the Treatment of Associated Bias. *Reliability Engineering and System Safety* 1993; 42(2-3):161-180.
23. Budnitz RJ, Apostolakis G, Boore DM, Cluff LS, Coppersmith KJ, Cornell CA, Morris PA. Use of Technical Expert Panels: Applications to Probabilistic Seismic Hazard Analysis. *Risk Analysis* 1998; 18(4):463-469.
24. Ayyub BM. *Elicitation of Expert Opinions for Uncertainty and Risks*. Boca Raton, FL: CRC Press 2001.
25. Cooke RM, Goossens LHJ. Expert Judgement Elicitation for Risk Assessment of Critical Infrastructures. *Journal of Risk Research* 2004; 7(6):643-656.
26. Cooke R. *Experts in Uncertainty: Opinion and Subjective Probability in Science*. Oxford; New York: Oxford University Press 1991.
27. Garthwaite PH, Kadane JB, O'Hagan A. Statistical Methods for Eliciting Probability Distributions. *Journal of the American Statistical Association* 2005; 100(470):680-700.
28. McKay MD, Beckman RJ, Conover WJ. A Comparison of Three Methods for Selecting Values of Input Variables in the Analysis of Output from a Computer Code. *Technometrics* 1979; 21(2):239-245.
29. Helton JC, Davis FJ. Latin Hypercube Sampling and the Propagation of Uncertainty in Analyses of Complex Systems. *Reliability Engineering and System Safety* 2003; 81(1):23-69.
30. Iman RL, Conover WJ. A Distribution-Free Approach to Inducing Rank Correlation Among Input Variables. *Communications in Statistics: Simulation and Computation* 1982; B11(3):311-334.
31. Iman RL, Davenport JM. Rank Correlation Plots for Use with Correlated Input Variables. *Communications in Statistics: Simulation and Computation* 1982; B11(3):335-360.
32. Helton JC. Uncertainty and Sensitivity Analysis Techniques for Use in Performance Assessment for Radioactive Waste Disposal. *Reliability Engineering and System Safety* 1993; 42(2-3):327-367.



33. Hamby DM. A Review of Techniques for Parameter Sensitivity Analysis of Environmental Models. *Environmental Monitoring and Assessment* 1994; 32(2):135-154.
34. Saltelli A, Chan K, E.M. Scott (eds). *Sensitivity Analysis*. New York, NY: Wiley, 2000.
35. Frey HC, Patil SR. Identification and Review of Sensitivity Analysis Methods. *Risk Analysis* 2002; 22(3):553-578.
36. Cacuci DG, Ionescu-Bujor M. A Comparative Review of Sensitivity and Uncertainty Analysis of Large-Scale Systems--II: Statistical Methods. *Nuclear Science and Engineering* 2004; 147(3):204-217.
37. Ionescu-Bujor M, Cacuci DG. A Comparative Review of Sensitivity and Uncertainty Analysis of Large-Scale Systems--I: Deterministic Methods. *Nuclear Science and Engineering* 2004; 147(3):189-2003.
38. Saltelli A, Ratto M, Tarantola S, Campolongo F. Sensitivity Analysis for Chemical Models. *Chemical Reviews* 2005; 105(7):2811-2828.
39. Helton JC, Johnson JD, Sallaberry CJ, Storlie CB. Survey of Sampling-Based Methods for Uncertainty and Sensitivity Analysis. *Reliability Engineering and System Safety* 2006; 91(10-11):1175-1209.
40. Helton JC, Davis FJ. *Sampling-Based Methods for Uncertainty and Sensitivity Analysis*. SAND99-2240. Albuquerque, NM: Sandia National Laboratories 2000.
41. Iman RL, Conover WJ. The Use of the Rank Transform in Regression. *Technometrics* 1979; 21(4):499-509.
42. Abdul Khader MH, Rao HS. Flow Through Annulus with Large Radial Clearance. *American Society of Civil Engineers, Journal of the Hydraulics Division* 1974; 100(HY1):25-39.
43. Feller W. *An Introduction to Probability Theory and Its Applications*, Vol. 2, 2nd edn. New York, NY: John Wiley & Sons, 1971.
44. Helton JC, Breeding RJ. Calculation of Reactor Accident Safety Goals. *Reliability Engineering and System Safety* 1993; 39(2):129-158.
45. Memorandum from K. Vierow, Chair, SOARCA Peer Review Committee to SOARCA Team through S. P. Burns, Re: Guidance on the SOARCA Uncertainty Quantification and Sensitivity Analysis, April 9, 2010.